Neural Mechanisms of Actions of Transcranial Electrical Stimulation

By

Kohitij Kar

A Dissertation submitted to the

Graduate School-Newark

Rutgers, The State University of New Jersey

in partial fulfillment of the requirements

for the degree of

Doctor of Philosophy

Graduate Program in Behavioral and Neural Sciences

written under the direction of

Bart Krekelberg

and approved by

_____

_____

_____

_____

_____

Newark, New Jersey

January 2015

Abstract of the Dissertation

Neural Mechanisms of Actions of Transcranial Electrical Stimulation

By Kohitij Kar

Dissertation Director:
Bart Krekelberg

There is considerable evidence for clinical and behavioral efficacy of transcranial electrical stimulation (tES). The effects range from suppressing Parkinsonian tremors to augmenting human learning and memory. Despite widespread use, the neurobiological mechanisms of action of tES on the intact human brain are unclear. In the work presented in this thesis, I have taken a multi-methodological approach to probe tES mechanisms. First, I studied the electric field spread induced by the application of tES, behaviorally. Second, I examined the behavioral effects of tES on human motion perception. I observed that tES (10 Hz, 0.5 mA) applied over area hMT+ (a brain area specialized in processing visual motion) attenuates motion adaptation. This result led to the hypothesis that tES-induced membrane voltage modulations reduce adaptation in motion-selective neurons. Finally, I tested this hypothesis by directly measuring tES-induced neural activity changes in a homologous area in the macaque brain (area MT). Tuning curve estimates of macaque MT neurons showed that tES attenuated the effects of visual motion adaptation on tuning amplitude and width. In addition to single cell measures, tES also significantly modified the evoked local field potentials. The results provide novel insights into how tES interacts with neural activity and establishes the awake, behaving macaque as an in-vivo animal model to study tES mechanisms.

Acknowledgements

"*Knowledge is in the end based on acknowledgement.*" Ludwig Wittgenstein

First, I express my deepest gratitude to Bart Krekelberg, my thesis advisor for his outstanding mentorship. Bart's highly accessible personality, his organization skills and his ability to be extremely meticulous without losing track of the bigger scientific picture, will remain with me as inspiration for years to come. I would like to thank the members of my thesis committee, Denis Pare, James Tepper, Farzan Nadim and Marc Sommer for their time and valuable inputs towards my thesis. I would also like to thank Ian Creese for being extremely helpful in the beginning of my coursework. Thank you for making me feel comfortable as a scientist amidst a pile of bureaucratic formalities. I would like to thank all former and current members of the Krekelberg Lab for their friendship and support throughout my PhD. Every lab meeting that ended in me thinking whether I am good enough, is the reason for every single useful outcome of my thesis work. I would like to thank all my friends and colleagues at the center of molecular and behavioral neuroscience, Rutgers- Newark for their support throughout my PhD, especially to Nur Zeynep Güngor. Zeynep, thank you for being there for me as a pillar of support in all the good and bad times. My life in USA wouldn't be so fulfilling if you never joined Rutgers. Last, but most importantly, I want to thank my parents and family, who supported me throughout these five years, from back home in India. It is just a great feeling to know that a few people exist with unconditional love and support, and you can always rely on them and go back to them for help.

Preface

The studies presented in chapters 2 and 3 have been published (Kar and Krekelberg, 2012; Kar and Krekelberg, 2014). Chapter 4 is currently under preparation for publication. Chapter 5 was a collaborative effort between myself and Jacob Duijnhouwer. The work has been submitted for publication and is currently undergoing the peer review process.

Table of Contents

List of Figures

List of Abbreviations

atDCS	Anodal Transcranial Direct Current Stimulation
BDNF	Brain Derived Neurotrophic Factor
BOLD	Blood Oxygen Level Dependent
ctDCS	Cathodal Transcranial Direct Current Stimulation
ECoG	Electrocorticography
EEG	Electroencephalography
HD	High Density
LFP	Local Field Potential
MEP	Motor Evoked Potential
MST	Middle Superior Temporal
MT	Middle Temporal
PSE	Point of Subjective Equality
rCBF	Regional Cerebral Blood Flow
RDK	Random Dot Kinematogram
RT	Reaction Time
TA	Tuning Amplitude
tACS	Transcranial Alternating Current Stimulation
tDCS	Transcranial Direct Current Stimulation
tES	Transcranial Electrical Stimulation
tRNS	Transcranial Random Noise Stimulation
TW	Tuning Width

CHAPTER 1

Introduction

1.1. Significance

Transcranial electrical stimulation (tES) has recently become a popular tool to noninvasively modulate brain activity for both clinical applications and cognitive neuroscience research (Utz et al., 2010; Zaghi et al., 2010). For instance, tES has been shown to aid treatment of therapy resistant depression (Palm et al., 2009), alleviate chronic pain (Antal et al., 2010), aid motor recovery after stroke (Schlaug et al., 2008), improve learning and memory (Kirov et al., 2009), numerical competence (Cohen Kadosh et al., 2010), reaction times (Hecht et al., 2010), cognitive aging (Meinzer et al., 2013; Kar and Wright 2014) and others. The evidence for its clinical and behavioral efficacy is overwhelming. However, given the rapidly growing literature on tES, it is surprising that there are so few studies directly addressing the neural mechanisms of action of tES. In fact, very little is known about how tES induce changes in neural activity in the intact human brain (Reato et al., 2013).

There have been a few attempts to understand the mechanisms of tES at the neural level. For instance, tES mechanisms have been studied in vitro, at the single cell level (Radman et al., 2009; Reato et al., 2010) and also in vivo (Ozen et al.,

2010; Ali et al., 2013). Another approach has been the finite element modeling of realistic human head models to predict the current distribution during application of tES (Datta et al., 2009). Despite these efforts, a parsimonious understanding of the mechanism of tES is lacking. I partially attribute these shortcomings to the lack of objective physiologically testable predictions from behavioral effects and a lack of in vivo models for tES.

The primary goal of the work presented in this thesis is to extend our understanding of the neural mechanisms of tES. First, I tested the current spread produced by tES as predicted by human head models (refer chapter 2). I then administered a behavioral test to estimate the cortical effects of tES and used qualitative models to generate testable neural hypotheses that can account for the behavioral effects (refer chapter 3 and chapter 4). Furthermore, I tested these predictions in vivo in an animal (macaque) model (refer chapter 5). In conjunction, the work presented in this thesis helps to develop a parsimonious understanding of the neural mechanisms of interaction of tES with the intact human brain. This will help optimize the use of tES in both basic science and clinical research.

1.2. Background of tES

Modes of transcranial electrical stimulation

There are three main modes of application of transcranial electrical stimulation. I will discuss each one separately in the following sections.

1. Transcranial direct current stimulation (tDCS)

Transcranial direct current stimulation is the most prevalent form of tES (Nitsche et al., 2008). In this method, a direct current is applied between two electrodes placed on the scalp of a human subject. The stimulation technique is often categorized as either anodal or cathodal (refer Figure 1.1). During an anodal stimulation, the positive electrode (anode) is placed over the area of the brain that is intended to be modulated by tDCS and the negative (cathode or reference) electrode is placed over an area that is not implicated in the behavioral task or experimental hypothesis and vice versa for cathodal stimulation. The electrodes are generally composed of conductive rubber pads placed over saline soaked sponges. A current density of around 0.02 – 0.08 mA/cm^2 is often used. The size and montage of the electrodes vary across studies (Bikson et al., 2012).

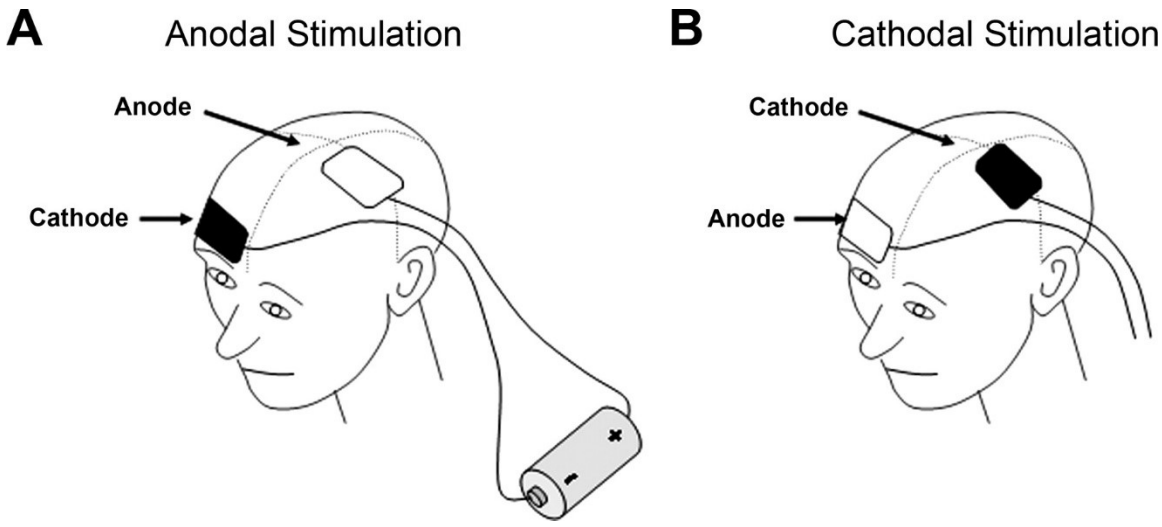

Figure 1.1 Demonstration of transcranial direct current stimulation of the motor cortex. A) Anodal stimulation of the left (pharyngeal) motor cortex. Anode placed over the motor cortex (left hemisphere) and cathode placed over the contralateral supraorbital ridge. B) Cathodal stimulation of the left (pharyngeal) motor cortex. Anode and cathode positions are swapped with regard to A). For tACS and tRNS the electrode montages are very similar. The difference lies in the type of current waveform passed through the electrodes. The figure has been adapted from (Jefferson et al., 2009).

2. Transcranial alternating current stimulation (tACS)

Transcranial alternating current stimulation is a variant of tDCS where the amplitude of current waveform passed across the two electrodes varies sinusoidally over time. This gives the experimenter the advantage of stimulating at multiple frequencies. I have used tACS in my thesis work as the primary mode of stimulation. The frequency tuning of tACS-induced behavioral effects is reported in chapter 4.

3. Transcranial random noise stimulation (tRNS)

In this mode, the intensity of current delivered to the human scalp across the two electrodes at any given time point is drawn from a random normal distribution with a selected mean current intensity (Yamamoto et al., 2005; Terney et al., 2008). The mean and the standard deviation of the underlying applied current distribution can be varied as parameters of tRNS. The frequency at which the current intensity changes value and a new value is drawn from the distribution can also be varied. This allows the experimenter to stimulate at different frequencies.

Electrode montages used in tES

Three most commonly used montages are the rectangular (or round) pads, high density (HD) 4x1 Ring montage and the concentric ring montage (Figure 1.2). In each of these montages, the current is passed between two electrodes (anode and cathode) connected to a current source. The number, shape and size of these electrodes vary to produce different montages. For instance, standard size for rectangular pads are 35cm^2, whereas each HD electrode is around 25 ± 2.5 mm^2 in size. In the work presented in this thesis, I have used round pads for the human psychophysics and rectangular pads for the monkeys. The shape of the electrodes were solely based on convenience, given the head shape and the area of interest (area MT).

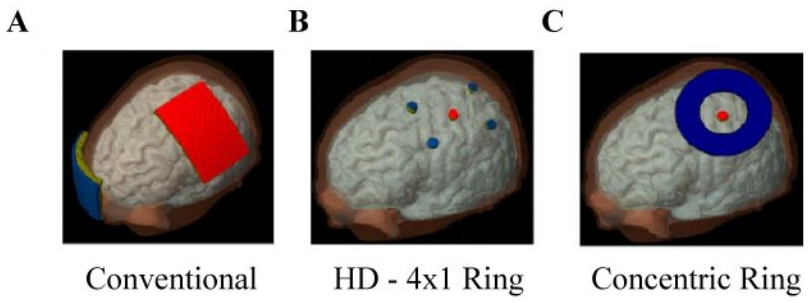

Figure 1.2 Common electrode montages used in tES. A) Conventional montage. tES is delivered across two rectangular (red and blue) pads (~ 35 cm^2). B) High density (HD) – 4x1 Ring. For anodal stimulation of an area, the positive electrode is placed at the center (area of interest) and the four negative electrodes are placed around it (vice versa for cathodal stimulation). C) Concentric rings (outer radius ranging 11–23 mm, inner radius: 9–21 mm). For anodal stimulation of an area, the anode is placed over the area whereas the cathode is placed as a concentric ring around the anode (vice versa for cathodal stimulation).

Methods of investigating the mechanisms of tES

There are three primary ways in which the mechanism of tES has been investigated so far. First, detailed human head models have been reconstructed from magnetic resonance imaging data to predict the spatial distribution of the induced current during tES. Second, neural mechanisms have been predicted from behavioral effects of tES. Third, the effects of tES in vitro and in-vivo have been studied. Simulation of both behavior and neural activity (single neuron and networks) with the help of computational models has also helped to shape our understanding of tES mechanism. I will now discuss these studies in more details, link them with my experimental approach and emphasize how the work presented in this thesis adds to a better understanding of the mechanisms of action of tES.

1. Human head models.

Head models are primarily of two types. First, there are coarse head models where the skull, the cerebrospinal fluid and the brain are represented as concentric spheres (Stecker, 2005). The conductance of each layer is key in predicting the distribution of the applied electric field. These models can be solved analytically. The other type of head model considers detailed geometry of the subject's head obtained from structural MRI. Specialized software utilizing finite element methods are needed to solve for the current densities at each location of the brain (Wagner et al., 2007). These models can also generate predictions about the current spread during tES with different electrode montages (Bikson et al., 2012). Although more sophisticated models are being developed (Dmochowski et al., 2011), there is a need to empirically validate their predictions. In chapter 2, I have addressed this specific issue.

2. Behavioral effects of tES.

Behavioral effects of tES under specific electrode montages allow researchers to speculate about the underlying mechanisms. For instance, a study done by Kanai and colleagues (Kanai et al., 2008) suggests that tACS applied over the visual cortex can synchronize with the ongoing neuronal oscillations like alpha and beta. Furthermore, studies done in conjunction with transcranial magnetic stimulation (TMS) show that cathodal tDCS decreases excitability while anodal tDCS increases excitability of the cortical area underneath the respective stimulating electrode (Nitsche and Paulus, 2000). Specifically, NMDA receptors have been

implicated in the short term effects of tDCS (Liebetanz et al., 2002). tDCS has been shown to improve probabilistic classification learning when applied to the prefrontal cortex and thereby assumed to increase neural excitability (Kincses et al., 2004). tDCS has also been shown to increase slow oscillatory EEG activity during sleep, facilitating neural plasticity and thereby improving declarative memory (Marshall et al., 2006). These behavioral effects hint at neural mechanisms but generally lack a specific hypothesis that can be readily tested in an animal model. In chapters 3 and 4, I have presented behavioral effects of tES with testable neural hypotheses, which were specifically tested in an animal model in chapter 5.

3. Electrophysiological studies of tES mechanisms.

A study done in mouse M1 slices suggests that direct current stimulation can lead to long lasting synaptic potentiation (Fritsch et al., 2010) which is mediated by the brain derived growth factor (BDNF). Low intensity electrical stimulation (< 50 Hz) affects carbachol induced gamma oscillations in hippocampal slices (Reato et al., 2010). Radman et al. (2009) have characterized, in detail, the role of neuron type and morphology during uniform field stimulation of rat motor cortex brain slices (Radman et al., 2009). Human EEG recordings have suggested that 10 Hz tES increases alpha power and affects spike time dependent plasticity (Helfrich et al., 2014; Zaehle et al., 2010). Whether these observations are valid in the intact brain, remains to be tested. A few attempts have been made to develop in vivo models (Ozen et al., 2010; Ali et al., 2013). The main drawback of these approaches has been the direct linking of the inference of these studies with human subjects. For

instance, Ozen et al. (2010) directly stimulated the skull of rats entraining neural activity. Although this shows the capability of tACS to entrain neuronal activity, such a design is very different from the human tACS setup, given the absence of the skin tissues of the scalp. Furthermore, Ali et al. (Ali et al., 2013) studied anesthetized ferrets. Hence the inference drawn from the study about the potential effects of tACS in an intact awake human head is limited. The work presented in this thesis overcomes these limitations by using an awake, behaving macaque model (chapter 5).

1.3. Visual motion system: A model system to probe mechanisms of tES

I have specifically used the well explored visual motion area of the primate to probe the mechanism of tES in this thesis. The visual motion area has been identified and well characterized (Albright, 1984; Sunaert et al., 1999) in both humans (area hMT+) and macaques (area MT). There are well established homologies between human and macaque visual systems. Hence it is likely that the neural mechanisms that generate the behavioral results in humans can be directly investigated in the macaques. Apart from this, there are well defined objective measures to estimate motion sensitivity of human and non-human primate observers (Nishida, 2011).

1.4. Approach

In this thesis, I extend the current research on tES mechanisms in multiple ways. By using objective measures, I developed novel behavioral paradigms to study the

current spread during tES in human subjects (chapter 2). I generated testable neural predictions based on behavioral studies done by stimulating human brain areas, specifically the well explored area hMT+ (chapters 3 and 4). So far, the mechanistic understanding of tES was primarily based on in vitro studies. The key innovation in this thesis is to investigate the mechanisms of tES in awake, behaving monkeys. This allows us to compare the influence of tES on intracortical measures of neural activity (in macaque area MT; chapter 5) with behavioral changes (in humans, chapters 3 and 4).

CHAPTER 2

Transcranial electrical stimulation over visual cortex evokes phosphenes with a retinal origin

In this chapter, I present a novel behavioral method to predict the spread of applied electric fields during tES across the subjects' head. I provide empirical evidence that phosphenes (peripheral visual flickers) evoked by sinusoidal tACS applied over visual cortex are due to current spread to the retina and not a result of direct stimulation of the visual cortex. This chapter has been published in the journal of neurophysiology (2012).

Published journal article included in the chapter:

Kar, Kohitij, and Bart Krekelberg. "Transcranial electrical stimulation over visual cortex evokes phosphenes with a retinal origin." *Journal of neurophysiology* 108.8 (2012): 2173-2178.

2.1 Abstract

Transcranial electrical stimulation (tES) is a promising therapeutic tool for a range of neurological diseases. Understanding how the small currents used in tES spread across the scalp and penetrate the brain will be important for the rational design of tES therapies.

Alternating currents applied transcranially above visual cortex induce the perception of flashes of light (phosphenes). This makes the visual system a useful model to study tES. One hypothesis is that tES generates phosphenes by direct stimulation of the cortex underneath the transcranial electrode. Here, we provide evidence for the alternative hypothesis that phosphenes are generated in the retina by current spread from the occipital electrode.

Building upon the existing literature, we first confirm that phosphenes are induced at lower currents when electrodes are placed farther away from visual cortex and closer to the eye. Second we explain the temporal frequency tuning of phosphenes based on the well-known response properties of primate retinal ganglion cells. Third, we show that there is no difference in the time it takes to evoke phosphenes in the retina, or by stimulation above visual cortex.

Together, these findings suggest that phosphenes induced by tES over visual cortex originate in the retina. From this we infer that tES currents spread well beyond the area of stimulation, and are unlikely to lead to focal neural activation. Novel stimulation protocols that optimize current distributions are needed to overcome these limitations of tES.

2.2 Introduction

Transcranial electrical stimulation (tES) is a promising therapeutic tool in clinical trials involving posttraumatic stress, stroke recovery, depression and many other neurological diseases (http://clinicaltrials.gov/). While the acute effects of electrical fields in vitro are relatively well understood (Reato et al., 2010) , we have limited understanding how transcranial currents interact with neuronal dynamics in the intact brain. Kanai et al. (2008) argued that tES directly modulates neural activity underneath a stimulating electrode. They applied transcranial alternating current stimulation (tACS) over visual cortex and found that subjects reported seeing flashes of light (phosphenes). The subjective strength of these phosphenes depended on the temporal frequency of tACS and the light adapted state of the subject. Specifically, phosphenes were strongest for tACS at 10Hz (dark) but 20Hz (light). Kanai et al. interpreted this as showing that tACS could entrain the dominant brain oscillations in the dark (alpha) or the light (beta).

While this is an intriguing hypothesis, a number of objections have been raised to this interpretation (Schwiedrzik, 2009). First, there is convincing evidence that phosphenes can be induced by electrical stimulation of the retina. Brindley (1955) passed alternating current (0.03-0.7 mA) through bipolar electrodes placed directly on the conjunctiva, which reliably evoked the perception of phosphenes. Pressure blinding of the eye caused temporary blindness to both visual stimuli and electrically induced phosphenes. Brindley concluded that voltage changes induced directly in the photoreceptors were the most likely explanation of these

phosphenes. Schutter and Hortensius (2010) proposed that the supposed cortically evoked phosphenes reported by Kanai et al. could be due to volume conduction from the occipital electrode to the retina, evident in the voltage changes measured near the eye. Paulus has argued that those voltage changes were too small to evoke phosphenes (Paulus, 2010).

Resolving this long standing debate (Rohracher, 1935) and determining the origin of tES phosphenes has considerable implications for the ability of tES to modulate specific brain areas (or rhythms) in clinical and basic research. The cortical entrainment hypothesis claims that neural activity below a tES electrode can be modulated relatively easily. The retinal hypothesis, on the other hand, claims that while it is indeed easy to generate phosphenes with tES, these phosphenes do not result from the direct modulation of neural activity below the electrode. .

We combined experimental and computational methods to investigate the origin of tES induced phosphenes. We first use a novel paradigm to confirm that current thresholds for phosphenes decrease when electrodes are placed away from visual cortex and closer to the eye. This is expected for a retinal origin of phosphenes. Second, we show that the frequency tuning of these phosphenes can be understood from the basic response properties of retinal ganglion cells (Benardete and Kaplan, 1999). Finally, we show that there is no difference in the time it takes to evoke phosphenes by a single current pulse through an electrode near the eye, or near visual cortex. This is inconsistent with the cortical hypothesis because

phosphenes generated directly in cortex should be faster than retinal phosphenes by the typical response latency of V1 neurons. Taken together, our data strongly support the view that the origin of tES induced phosphenes is retinal.

2.3 Materials and Methods

Subjects

Six subjects (5 naïve and 1 experimenter; 5 subjects for the phosphene detection task, 4 subjects for the double pulse detection task) participated in the study. Subjects gave written consent and all had normal or corrected to normal vision. This study was conducted according to the principles expressed in the Declaration of Helsinki and approved by the Institutional Review Board of Rutgers University. S-4 is the non-naïve subject (experimenter KK).

Visual Stimuli

The phosphene detection and the double pulse detection task were done in a room lit only by the background luminance (0.4 cd/m^2) of a monitor (Sony FD Trinitron CRT monitor resolution of 1024 x 768 pixels; refresh rate of 120 Hz).

Apparatus

We used an STG4002 stimulus generator (Multi Channel Systems, Reutlingen, Germany) to deliver the transcranial electrical current stimulation. We used saline soaked sponges attached to conductive rubber as electrodes (3” diameter). All events in a trial were synchronized and triggered using in-house software,

Neurostim http://neurostim.sourceforge.net). A head-mounted Eyelink II eye tracker system (SR Research, Mississauga, Canada) recorded eye movements by tracking the pupils of both eyes at a sampling rate of 500 Hz.

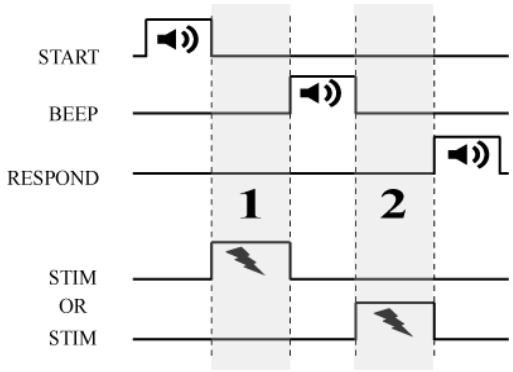

Figure 2.1 Design of the phosphene detection task. Trials consisted of two intervals (1 and 2) separated by a beep; tACS was applied in one of the two intervals. Subjects reported the interval in which they saw phosphenes and we determined the current level at which the subject's phosphene detection performance reached 75% correct.

Procedures

All subjects sat in a dark room at a distance of 57cm from the center of the monitor. Head movements were restricted by using a chinrest or a bite bar. The subjects indicated their response using the keyboard.

Electrode Placement

We placed the stimulating electrode at three regions of interest; the occipital lobe (Oz), the temporal lobe (T5) and the frontal lobe (Fpz) according to the international 10-20 system of electrode placement. The reference electrode was

always at the vertex (Cz). The maximum current density used was 0.02mA/cm^2 (current intensity = 1mA; electrode surface area = 45.6cm^2)

Phosphene Detection Task

This experiment was designed to determine the threshold intensity of stimulation to elicit phosphenes. The stimulation was limited to -0.5mA to 0.5 mA of sinusoidal current. We used 8, 10, 15, 20, 30 and 60 Hz as the tES frequencies. The voltage was limited to 20V. Each trial in the experiment began with a 'START' sound followed by two intervals of 1000 ms separated by a beep. Stimulation was delivered for the full duration of either of the two intervals and the subjects reported the interval in which they saw phosphenes. We used a Bayesian adaptive threshold estimation algorithm (Kontsevich and Tyler, 1999) to select the intensity of tES for each trial and defined threshold as the current at which the subjects' performance reached 75% correct. Subjects performed a minimum of 30 trials per condition (i.e. per montage and frequency).

Double Pulse Detection Task

This experiment was designed to estimate the time interval required to perceive two phosphenes when two electrical pulses were applied in succession. Subjects fixated a small dot on an otherwise dark screen. All trials in which the subjects broke fixation from a 2^o x 2^o window were discarded from the analysis. After a 'START' sound to indicate the beginning of the trial, we applied two 20ms unipolar electrical pulses and varied the onset time between the pulses (dt) over a range of 20 to 160 ms. One pulse was applied at the frontal electrode (Fpz), the other at the

occipital electrode (Oz). Catch trials containing only a single pulse were randomly interleaved. To create phosphenes with approximately equal perceived brightness, we adjusted the currents at the Oz and Fpz electrodes. Specifically, we determined the average (across subjects and frequencies) ratio of the threshold currents in Experiment 1, chose a suprathreshold current value for Fpz (0.3mA) and, using the ratio (3.2), calculated 1mA as the current for the Oz electrode.

We determined subjects' sensitivity (d') as:

$$d' = \text{norminv}(HIT) - \text{norminv}(FA)$$

where the hit rate (HIT) is the fraction of trials in which the subject reported perceiving both of the two applied pulses, and the false alarm rate (FA) is the fraction of trials in which one pulse was applied, but the subject reported perceiving two pulses. norminv(.) denotes the inverse of the cumulative normal distribution. We fitted a straight line to d' as a function of dt and estimated the threshold delay as the delay required to achieve a sensitivity d' of 1.5.

To test whether threshold delays were significantly different in the two conditions, we performed a permutation test of the null hypothesis that the Oz-Fpz and Fpz-Oz data belonged to the same distribution (Efron and Tibshirani, 1994). In this procedure we combined the responses from all Fpz-Opz and Oz-Fpz trials, drew (with replacement) two complete datasets from this distribution, and determined the difference in threshold delays. We repeated this resampling process 1000 times to obtain a null distribution of threshold delay differences. We then determined the p-value of the test as the fraction of values in the null distribution

that were larger than the actual difference in threshold delay between the Fpz-Oz and Oz-Fpz experimental data (Efron and Tibshirani, 1994).

Because the retinal hypothesis predicts that the threshold delays are *not* different, we wanted to be sure that our test had sufficient power to detect differences in delays if they existed. Therefore, we determined the power of the permutation test. The power is defined as one minus the probability that the test failed to detect a significant difference if the cortical hypothesis were correct. Specifically, we calculated the probability that the observed latency differences could come from a distribution of latency differences with a mean equal to the expected effect size under the cortical hypothesis ($2*\Delta v_1$ = 120ms) and a standard deviation given by the error in our estimate of the threshold. We determined the latter by bootstrap resampling (N=1000) the individual subject data (Efron and Tibshirani, 1994). The values of the power for subjects S-3, S-4, S-5 and S-6 were 0.87, 0.86, 0.98, and 0.81 respectively.

Retinal Ganglion Cell Model

To investigate whether known properties of retinal ganglion cells could quantitatively explain the frequency tuning of phosphene current thresholds, we adapted the linear cascade filter model proposed by Victor (1987). Bernadette and Kaplan estimated the parameters of the model by recording from macaque retinal ganglion M cells (Benardete and Kaplan, 1999). In the model, the firing rate of each retinal ganglion cell (RGC) depends on visual contrast(c) and stimulation frequency ($f = \frac{\omega}{2\pi}$).

$$R(\omega, c) = A * e^{i\omega D}\left(1 - \frac{Hs}{1 + i\omega\tau_s(c)}\right)\left(\frac{1}{1 + i\omega\tau_L}\right)^{N_L}$$

$$\tau_s(c) = \frac{T_o}{\left(1 + \left(\frac{c}{C_{1/2}}\right)^2\right)}$$

where, A is overall gain per unit contrast (impulses/s-u.c.), D is initial delay (ms), Hs is strength of the high pass filter, τ_s is time constant of the high pass stage (ms), τ_L is time constant of the low pass stage (ms), T_o is time constant of high pass stage for zero contrast (ms), $C_{1/2}$ is contrast at which τ_s is half its initial value and N_L is approximate number of low pass filters.

We supplemented this RGC model with a front-end and a back-end. The front-end modeled the relationship between the stimulation current, I and the effective visual contrast, c(M) for montage M as:

$$c(M) = I^{\beta}/\delta(M)$$

where β is a scaling parameter and δ is the equivalent electrotonic distance between the eyes and the stimulating electrode for montage M. Note that β and δ were not measured directly; they were estimated from the behavioral responses using an optimization procedure (see below). We furthermore assumed that detection performance was a Weibull function of the retinal ganglion cell's firing rate, R (back-end).

$$P = g\ (\xi, \theta, R(\omega, c))$$

where P is the predicted fraction correct, g is a Weibull function and θ and ξ are the threshold and slope of the sigmoid psychometric function, respectively. Note that none of these assumptions about the front- or back-end of the model introduce frequency tuning; all frequency tuning in the model arises from the properties of the RGCs.

The model predicted the fraction correct for any stimulation current and frequency. Using Matlab's *fmincon,* we varied the four free model parameters (β, δ, ξ , θ) and the constrained RGC parameters to obtain the best fit of the complete psychometric function (3 montages, 4 temporal frequencies, and a large number of current intensities; not just the threshold) for each subject. The values of the RGC model parameters were constrained to fall within the range estimated for primate ganglion cells by Benardete and Kaplan (1999). In other words, each model contained RGCs whose properties were within the measured range of macaque ganglion cells.

2.4 Results

When stimulated with a weak alternating current through a primary electrode placed on the occipital pole (Oz) and a reference electrode on the vertex (Cz), subjects report perceiving a widely distributed peripheral flicker whose temporal frequency varies with stimulation frequency (Rohracher, 1935; Brindley, 1955; Kanai et al., 2008). The subjective brightness of this flicker increases when the

first electrode is placed more anterior. This property of tACS induced phosphenes has been known for some time (Rohracher, 1935) and is inconsistent with the cortical hypothesis, but strongly suggests a retinal origin.

Phosphene Thresholds

To measure these phenomena in an objective manner, we used a two interval forced choice task (Figure 2.1), and an adaptive method to determine current levels required to reliably evoke phosphenes from electrodes placed over the occipital lobe (Oz), temporal lobe (T5), or frontal lobe (Fpz), each with a reference on the vertex (Cz). Figure 2.2 shows data from all subjects. The current thresholds decreased for electrodes closer to the eye and therefore further away from the visual cortex. This supports the view that the phosphenes originate in the eye, and not from direct stimulation of the cortex.

Frequency Tuning

Figure 2.2 also shows that the phosphene thresholds were tuned for the temporal frequency of stimulation. This feature has previously been attributed to the entrainment of cortical oscillations (Kanai et al., 2008). We investigated whether this temporal frequency tuning could instead be interpreted in terms of retinal response properties. Qualitatively, this interpretation is supported by the fact that retinal ganglion cells have a temporal frequency tuning with peak sensitivity in the alpha range in the dark; see for instance Figure 1 in (Benardete and Kaplan, 1999). Moreover, the peak sensitivity of retinal ganglion cells shifts towards the beta

frequency band in the light (Purpura et al., 1990), which matches the shift in the optimal stimulation frequency for phosphenes in a lit room (Kanai et al., 2008).

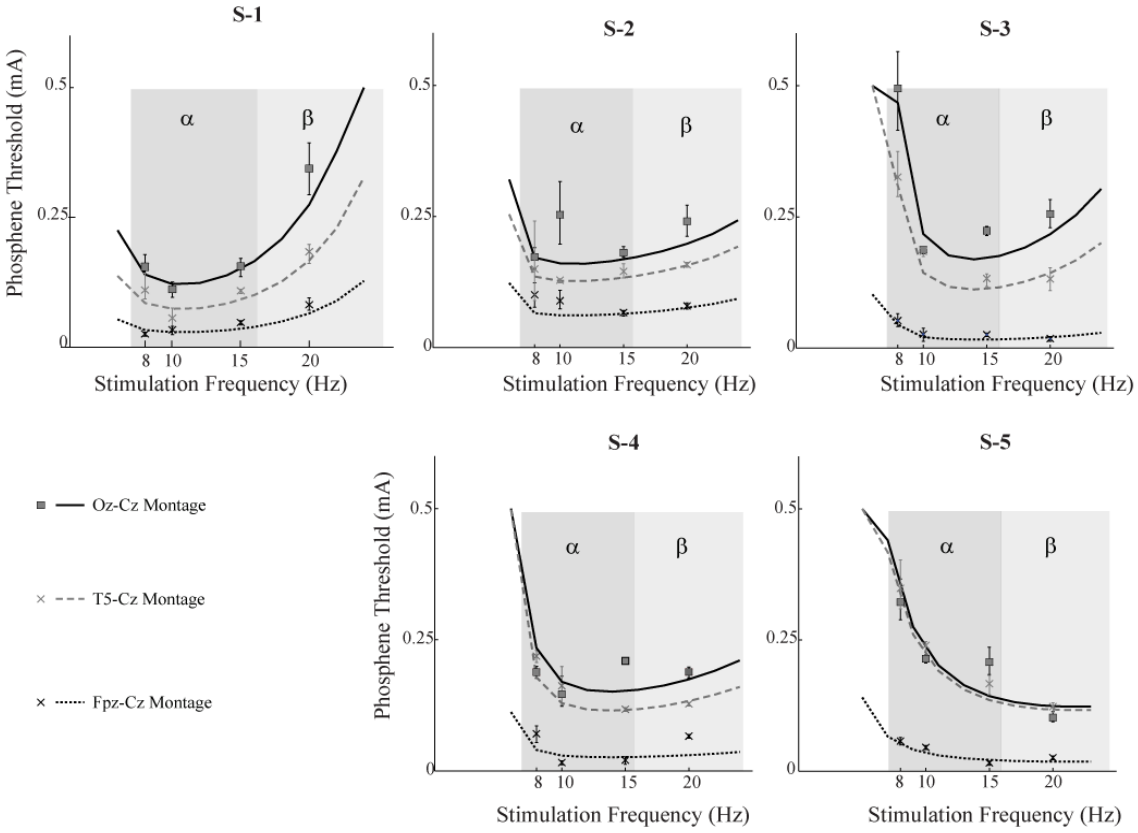

Figure 2.2 Threshold measurement and frequency tuning. Dependence of phosphene thresholds on stimulation frequency (8-20 Hz) and electrode position for five subjects (S-1, S-2, S-3, S-4, S-5). The α and β frequency bands are shaded in dark and light grey respectively. Consistent with the findings of Kanai et al, the optimal stimulation frequency for these experiments done in near darkness was typically in the alpha range. The box and 'x' markers are the estimated thresholds; error bars indicate 95% confidence intervals and the lines represent the model fit based on the Retinal Ganglion Cell model. The figure shows that current thresholds decreased as the electrode was moved closer to the eye; consistent with a retinal origin. Moreover, it shows that the temporal frequency tuning is consistent with the known properties of primate retinal ganglion cells.

To provide quantitative support for the match between phosphene thresholds and retinal ganglion cell properties, we used a well-established model for retinal ganglion cells (Victor, 1987). This model provides a quantitative description of the relation between visual contrast and the firing rate of retinal ganglion cells, including their temporal frequency tuning.

We developed a simple, descriptive front-end to this model to relate tES stimulation current (the independent variable in our study) to the effective visual contrast generated at the retina (the input to the RGC model). Specifically, we assumed that the effective visual contrast decreased with the electrotonic distance between the electrode and the eye. The parameters describing this decrease were estimated from the data. Similarly, we added a descriptive back-end to the RGC model that described how firing rate was related to behavioral performance (See methods). The parameters of the front and back-end were unconstrained, and determined by optimization to produce the best fit to the individual performance curves. The parameters of the RGC model, however, were constrained to lie within the ranges measured in the primate retina (Benardete and Kaplan, 1999).

The curves in Figure 2.2 show the best fits of the model to the individual subject data (For details, see Methods). We could not estimate the thresholds at stimulation frequencies of 30Hz and higher as they were above the pre-determined range of our current stimulation amplitude (0.5mA); we did not use those data for the model fits. Note however, that this implies that thresholds above 30Hz were at

least 0.5mA, hence all subjects had U-shaped response curves, as expected qualitatively from the RGC properties.

Double Pulse Detection Task

When a single 20ms pulse of 1mA was applied to the occipital lobe (Oz), subjects reliably reported seeing a brief flash of peripheral light. On the one hand, this shows that entrainment of cortical oscillations is not necessary to evoke phosphenes from an electrode on the occipital lobe. But, more importantly, it provides us with a tool to determine whether currents injected at the occipital lobe spread to the eye.

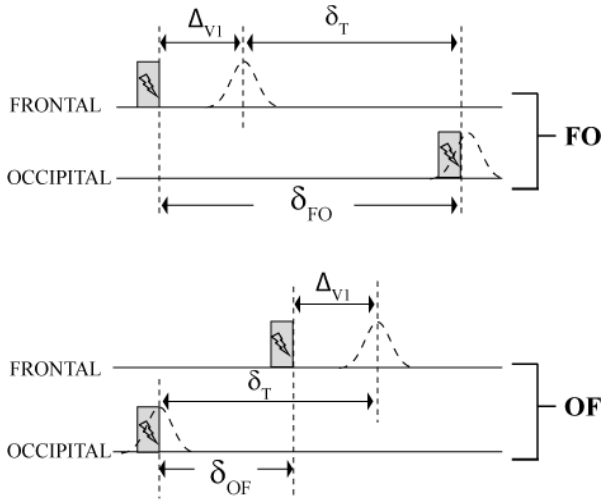

Figure 2.3 Predictions for the double pulse detection task based on the hypothesis that occipital stimulation evokes neural activity directly in the underlying cortex. Grey bars represent the stimulation; dashed curves the activity in V1 under the cortical hypothesis. This panel illustrates why the cortical hypothesis predicts large differences in the time needed to distinguish two phosphenes between OF and FO stimulation. See main text for a full description.

A single pulse through a frontal electrode (Fpz) also evokes a phosphene, and it is generally accepted that these phosphenes have a retinal origin

(Rohracher, 1935; Brindley, 1955). We asked whether the phosphene evoked by occipital stimulation could have a direct cortical origin instead. The distinguishing feature we use is that retinal stimulation –unlike direct cortical stimulation– requires some time to reach visual cortex. We call this latency Δ_{V1} and we estimate it as ~60ms based on EEG data (Jeffreys and Axford, 1972). In the experiment, we applied one frontal pulse (Fpz) and one occipital pulse (Oz) and asked the subjects to report whether they saw one or two pulses.

To perceive two phosphenes requires a minimum time (δ_T) between the two corresponding bursts of neural activity in visual cortex. Under the cortical hypothesis, the current pulses in an Fpz-Oz sequence (Figure 2.3) would have to be apart by $\delta_{FO} = \delta_T + \Delta_{V1}$ to create V1 activity separated by δ_T. In an Oz-Fpz sequence, however, the Oz pulse gets a head start, hence the current pulses would only have to be $\delta_{OF} = \delta_T - \Delta_{V1}$ apart. Under the retinal hypothesis there is no difference between the conditions because both phosphenes originate at the retina with negligible time delays due to electrical conduction from Oz to Fpz.

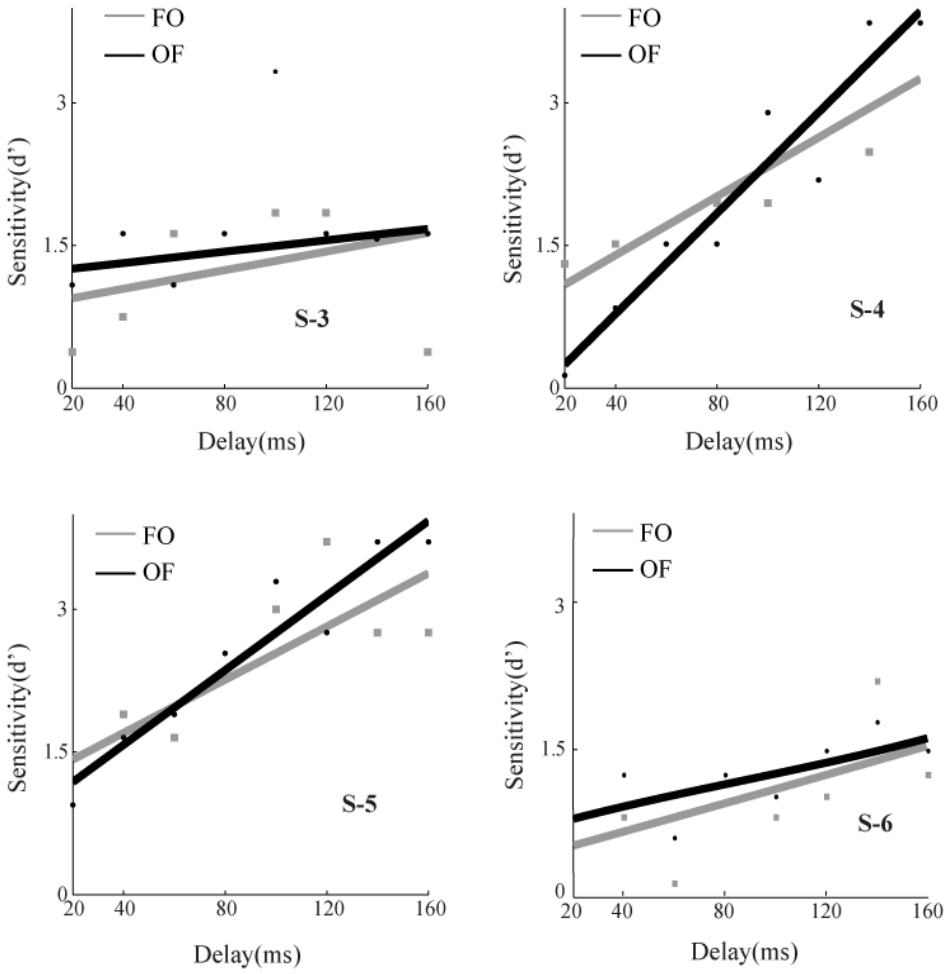

Figure 2.4 Double-pulse detection sensitivity. Behavioral report for four subjects (S-3, S-4, S-5 and S-6) in the double pulse detection task. The sensitivity (d') of the subject to detect two flashes is shown as a function of the time between the two stimulation pulses. The bold lines are lines fitted to the data points. Threshold delay is defined as the delay at which the sensitivity (d') reached 1.5. The threshold delays for Oz-Fpz and Fpz-Oz conditions were statistically indistinguishable for all subjects (Permutation test; $p>0.05$).

Figure 2.4 shows the sensitivity to detect two pulses using the signal detection measure d'. As expected, sensitivity to detect two pulses increased with the delay between the pulses. Importantly, sensitivity for Oz-Fpz sequences was

indistinguishable from sensitivity for Fpz-Oz sequences. Statistically, none of the subjects had a significant difference between the minimal delay needed to reliably (d'=1.5) distinguish two pulses in the Oz-Fpz and Fpz-Oz sequences. This is consistent with the retinal hypothesis. The cortical hypothesis on the other hand predicts that these curves should be shifted laterally by $2*\Delta v_1 \approx 120$ms. We used this estimate of the expected effect to determine the statistical power of our test (See Methods); the power was above 0.8 for each subject. Hence, our data do not allow us to reject the null hypothesis that the phosphenes have the same source, and this is not likely to be due to a lack of power in the statistical analysis. We infer that Oz and Fpz stimulation have the same source. Because Fpz stimulation is generally agreed to have a retinal origin (Rohracher, 1935; Brindley, 1955), we conclude that Oz stimulation does too.

2.5 Discussion

We investigated the origins of phosphenes induced by transcranial electric stimulation. Consistent with the previous literature (Rohracher, 1935; Schutter and Hortensius, 2010), we found that phosphene thresholds increased with the distance between the electrodes and the eye. Furthermore, we showed that the temporal frequency tuning of current thresholds is consistent with the known properties of retinal ganglion cells. And finally, we found no difference in the time it takes to elicit a phosphene by stimulating over visual cortex compared to frontal cortex, even though a direct cortical effect of electrical stimulation predicts a time

difference as large as 120ms. Taken together, these data strongly argue that tACS-induced phosphenes originate in or before retinal ganglion cells and are unlikely to be caused by the entrainment of cortical oscillations (Kanai et al., 2008).

We will first discuss the possible mechanisms underlying phosphene generation in the retina, and then the implications of our findings for the use of tES in clinical applications and basic research.

Within the retina, several mechanisms could contribute to the generation of phosphenes by the application of electrical fields (Attwell, 2003). Clinical observations help to narrow down the likely locus for phosphene generation by tACS. For instance, electrical stimulation of the conjunctiva induces phosphenes even in patients with damaged photoreceptors (*retinitis pigmentosa* or *ablatio retinae)* and in these patients the frequency tuning of the phosphene threshold is preserved (Meier-Koll, 1973). Frequency tuning is lost, however, in patients whose optic nerve is severed, or those in which occluded blood vessels lead to the degeneration of bipolar and ganglion cells, e.g. in *retinopathia diabetic,* (Meier-Koll, 1973) . Given that models of volume conduction in the human head predict that tES can generate high current densities in the optic nerve, stimulation of the axons of RGCs is a candidate mechanism. However, pressure blinding abolishes phosphenes generated by direct stimulation of the cornea (Brindley, 1955). Because pressure blinding is unlikely to affect the optic nerve, Brindley concluded from this observation that electrical stimulation directly affects the photoreceptors.

More recently, it has been shown that direct electrical stimulation of the optic nerve of a blind patient with severe retinitis pigmentosa (Delbeke et al., 2003) resulted in phosphenes without the typical band-pass temporal frequency tuning shown in Figure 2.2. While invasive experiments may be needed to answer this mechanistic question conclusively, these observations strongly suggest that the characteristic frequency tuning found in tES originates before the optic nerve.

Our experiments used objective measures of phosphene detection. This minimized the influence of observer bias and avoided relying on the subjective report of observers' phenomenal experience, which we found to be variable across subjects and somewhat difficult to describe. This ephemeral quality of the phosphenes makes it difficult to compare the effect of electrical stimulation with matched visual stimuli. Informal experiments showed that most visual stimuli mask tES induced phosphenes more effectively than tES phosphenes mask visual stimuli. However, this finding is difficult to interpret quantitatively as any visual property that was not matched between the stimuli could contribute to this asymmetry. For instance, the phosphenes extended farther into the periphery and had a subjectively weaker appearance than any visual stimulus we could present. An additional explanation for this asymmetry is that tES polarizes the membrane of photoreceptors only transiently, while the signaling cascade started by light, typically changes the membrane for a much longer period of time (Baylor et al., 1984; Schneeweis and Schnapf, 1999).

Our claim is not that transcranial stimulation cannot affect the brain. Given enough current, it is inevitable that an electrode placed on the scalp will modulate brain activity. Moreover, recent studies suggest that even at low current levels tACS can entrain EEG signals (Polania et al., 2012). This does not imply, however, that tACS entrainment of cortical oscillations plays a causal role in the induction of phosphenes. First, we have shown that even a single 1mA pulse over visual cortex can evoke a phosphene. This shows that synchronization with ongoing oscillations is not necessary. Second, we have provided a novel interpretation of the temporal frequency tuning of phosphenes in terms of the the well-known physiological properties of retinal ganglion cells. The conclusion we draw from these findings is that there is no convincing evidence that tES modulates neural activity underneath the electrode enough to generate a percept.

The broader conclusion we draw is that currents induced at the occipital pole spread widely across the scalp; well beyond the location of the electrode, and outside the direct path between electrode and reference. This is consistent with predictions of detailed models that simulate the current spread in the human head during tDCS (Datta et al., 2009). Taken together these findings imply that tES in its current form is unlikely to lead to focal neural activation. Transcranial electrical stimulation in a therapeutic setting would benefit from the ability to target specific areas, hence novel stimulation protocols that optimize current distributions (Dmochowski et al., 2011) are needed to overcome this limitation.

CHAPTER 3

Transcranial alternating current stimulation attenuates visual motion adaptation

In chapter 2, I concluded that during the application of tACS, the electric field induced in the subject's head, spreads well beyond the area of application due to volume conduction. Taken together with predictions from theoretical models of tACS-induced current distribution in human head (Bikson et al., 2012), it is likely that tACS only has subthreshold effects (if any) at the cortical level. This leads us to the question whether tACS applied over a brain area can induce any significant behavioral effect by selectively modulating the underlying cortex. I specifically address this question in this chapter. I present conclusive evidence for the cortical effects of tACS and generate testable mechanistic predictions. This chapter has been published as a journal article in the Journal of Neuroscience, 2014.

Published journal articles included in the chapter:

Kar, Kohitij, and Bart Krekelberg. "Transcranial Alternating Current Stimulation Attenuates Visual Motion Adaptation." The Journal of Neuroscience 34.21 (2014): 7334-7340.

3.1. Abstract

Transcranial alternating current stimulation (tACS) is used in clinical applications and basic neuroscience research. Although its behavioral effects are evident from prior reports, current understanding of the mechanisms that underlie these effects is limited. We used motion perception, a percept with relatively well-known properties and underlying neural mechanisms to investigate tACS mechanisms.

Healthy human volunteers showed a surprising improvement in motion sensitivity when visual stimuli were paired with 10 Hz tACS. In addition, tACS reduced the motion-after effect, and this reduction was correlated with the improvement in motion sensitivity. Electrical stimulation had no consistent effect when applied before presenting a visual stimulus or during recovery from motion adaptation. Together, these findings suggest that perceptual effects of tACS result from an attenuation of adaptation.

Important consequences for the practical use of tACS follow from our work. First, because this mechanism interferes only with adaptation, this suggests that tACS can be targeted at subsets of neurons (by adapting them), even when the applied currents spread widely throughout the brain. Second, by interfering with adaptation, this mechanism provides a means by which electrical stimulation can generate behavioral effects that outlast the stimulation.

3.2. Introduction

There is rapidly growing interest in using transcranial alternating current stimulation (tACS) to modulate brain activity in both clinical applications and cognitive neuroscience research (Utz et al., 2010; Zaghi et al., 2010). For instance, tACS has been claimed to suppress Parkinsonian tremors (Brittain et al., 2013), entrain motor performance (Joundi et al., 2012), aid recovery after stroke (Schlaug et al., 2008; Fedorov et al., 2010), and improve learning and memory (Kirov et al., 2009), to name just a few. The mechanisms that underlie these long-term effects, however, remain poorly understood (Reato et al., 2013) .

Even though applied fields clearly modulate membrane polarization (Radman et al., 2009), the long-term effects of electrical stimulation may not be the direct consequence of this polarization, but the indirect consequence of changes in plasticity induced by the stimulation (Rosenkranz et al., 2000; Antal et al., 2004; Fricke et al., 2011; Antal et al., 2012). We used visual motion discrimination in humans to investigate this view. This model system has the advantage that its neural mechanisms are relatively well understood (Krekelberg, 2008a), that a specific cortical area (hMT+) has been identified to play a critical role (Sunaert et al., 1999), and that a large arsenal of objective measures for behavioral report are available for its study (for review see Nishida, 2011).

We first hypothesized that direct, tACS-induced perturbations should generate impairments in motion discrimination, because such perturbations are uninformative with respect to the direction of visual motion. Our experiments

rejected this hypothesis; instead we found that subjects were better at motion direction discrimination during the application of tACS. Puzzled by this unexpected improvement in performance we hypothesized that tACS could have prevented the reduction in motion discrimination performance that has previously been reported to occur for prolonged stimulus presentations (Van Wezel and Britten, 2002).

In a second set of experiments we tested this hypothesis using a standard motion adaptation paradigm (Hiris and Blake, 1992; Blake and Hiris, 1993). In such paradigms, a few seconds of exposure to, for instance, an upward moving pattern generates the illusory percept of downward motion in a subsequent stationary or random motion stimulus. As alluded to above, adaptation also typically reduces motion discrimination performance (Van Wezel and Britten, 2002). The behavioral effects of motion adaptation have been linked to neural adaptation in the middle temporal area (Kohn and Movshon, 2004; Krekelberg et al., 2006b), and the time scale at which these effects persist (tens of seconds) suggest that they rely on plastic changes such as synaptic depression, or long-term after hyperpolarization (Kohn, 2007). Consistent with our hypothesis, the experiments confirmed that tACS during the presentation of the visual motion stimulus (i.e., during the induction of adaptation) attenuated motion adaptation.

Taken together our experiments suggest a novel mode of action of tACS; the attenuation of adaptation. In the discussion we address the implications of these findings for using tACS and speculate about the underlying neural mechanisms.

3.3. Materials and Methods

Electrode Placement

One electrode was placed above the canonical location of left hMT+; PO7-PO3 in the 10-20 system. The other electrode was placed on the vertex (Cz). In the main experiments the parietal electrode was contralateral to the visual stimuli. In the ipsilateral control experiments, the electrode was placed above the hMT+ that was ipsilateral to the visual stimuli.

Subjects

Fifteen subjects participated in the experiments (eight female; fourteen naïve and one experimenter in total; 9subjects for the motion discrimination task, 10 subjects for the motion adaptation task, 10 subjects for the recovery task and 8 subjects for the pre stimulus tACS task). They gave written consent and had normal or corrected to normal vision. This study was conducted according to the principles expressed in the Declaration of Helsinki and approved by the Institutional Review Board of Rutgers University.

Apparatus

tACS was delivered through a STG4002 stimulus generator (Multi Channel Systems, Reutlingen, Germany). The stimulating electrodes were prepared as saline soaked sponges attached to conductive rubber electrodes (3" diameter). We used a sinusoidal current (1 mA peak to peak) at a frequency of 10 Hz. For safety reasons, the maximum voltage to produce the transcranial current was limited to

20V. The maximum current intensity was 0.5 mA and the electrode surface area was 45.6cm^2. All eye movements were recorded using an eye tracker (Eyelink II V 2.2) at 500 Hz. Stimulus presentations and the triggering of stimulation were under the control of Neurostim (http://neurostim.sourceforge.net).

Visual Stimuli

Stimuli were presented on a CRT monitor (Sony FD Trinitron) with a resolution of 1024 x 768 pixels at a refresh rate of 120 Hz. The main motion stimulus was a dynamic random dot kinematogram (RDK) consisting of 700 dots with an infinite lifetime and an effective diameter of 1.5 pixels using spatial dithering (OpenGL point size of 1.5). The dots were restricted inside a circular aperture of radius 5^o centered 7^o to the left or right of the center of the screen. The luminance of the dots was 30 cd/m^2, the background 0.4 cd/m^2. The dots moved at a constant speed of 3^o/s except during the speed change detection task (used to control for attention during adaptation; see below) when they moved at 6^o/s for a brief (200ms) period of time. We refer to the percentage of dots moving in the same direction (positive coherence: up, negative coherence: down) as the coherence. The remainder of the dots moved in randomly chosen directions. Stimuli such as these are commonly used to quantify motion perception (Newsome and Pare, 1988; Scase et al., 1996).

The RDK was used to construct the following five types of motion stimuli:

Long Adapter: RDK with dots moving upward with a coherence of 100% for 40 seconds.

Top-up Adapter: RDK with dots moving upward with a coherence of 100% for 4 seconds.

Test: RDK with different levels of coherence, presented for 1 second.

Long Test: RDK with different levels of coherence, presented for 4 seconds.

Random: RDK with all dots moving in a randomly chosen direction (0% coherence).

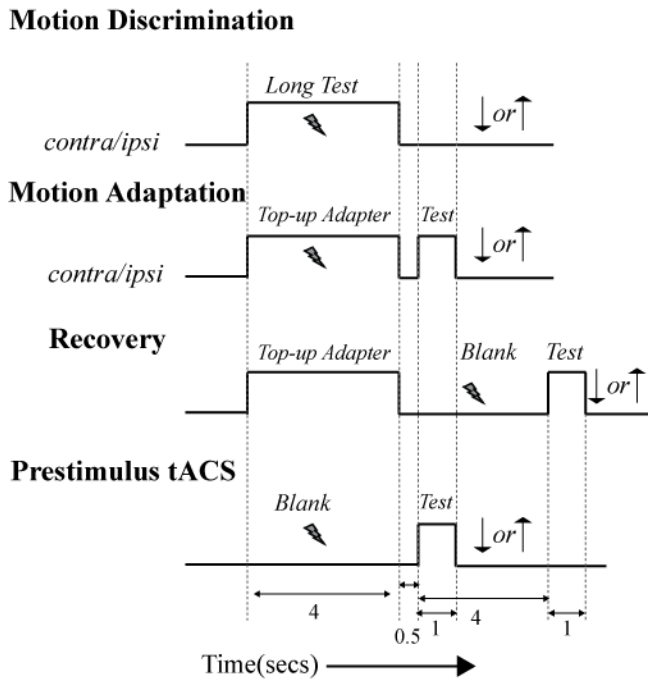

Figure 3.1 Summary of experimental paradigms (for details see Methods). The lightning bolt represents the application of tACS. In each paradigm subjects indicated the perceived direction of motion of the 'Test' stimulus by pressing the up (↑) or down (↓) button.

Experimental Procedures

Subjects were seated in a dark room at a distance of 57cm from the center of the monitor. Head movements were restricted by a molded bite bar. The subjects indicated their response using the keyboard. Fixation of a central red dot was monitored and trials in which the eye strayed beyond a virtual window of 2 degree were discarded.

Because transcranial electrical stimulation has been shown to have long lived effects (Nitsche and Paulus, 2001; Bolzoni et al., 2013), experimental conditions with and without stimulation could not be interleaved. The minimal time to start blocks of trials without stimulation after tACS had been administered for any paradigm was 24 hours.

Behavioral Tasks

In each of the experiments, the subjects' task was to indicate the perceived global direction of motion of the 'Test' stimulus: up or down (Figure 3.1).

Paradigm 1.Motion Discrimination

This paradigm served to measure the instantaneous influence of tACS on coarse motion discrimination. Eight subjects participated in the experiment. We presented the 'Long Test' stimuli and the subjects indicated the perceived global direction of motion (up or down). The coherence of the 'Long Test' stimuli ranged from -100% (all dots moving down) to +100% (all dots moving up). Stimulation was applied over the left hMT+ only during the presentation of the 'Long Test' stimuli. In

separate sessions, the visual stimulus was either presented in the right hemifield (contralateral condition) or left hemifield (ipsilateral condition).

Paradigm 2. Motion Adaptation

This paradigm measured the influence of tACS on the induction of adaptation using a standard top-up design. Each experimental session started with a single, 40s presentation of the 'Long Adapter' stimulus. In all subsequent trials the 'Top-up Adapter' stimulus (4s) was followed by a blank period (500ms) and then by the 'Test' stimulus (1s). The subject's task was to indicate the coherent motion direction of the 'Test' stimulus.

In the stimulation conditions, we applied tACS only when the 'Long Adapter' or 'Top-up Adapter' stimulus was on the screen. In the no-tACS conditions, no stimulation was applied. For the contralateral and ipsilateral experiments we stimulated the left hemisphere while showing the stimulus on the right hemifield and left hemifield, respectively.

To monitor and control the allocation of attention, subjects were instructed to attend to the adapter stimulus and press a key when a brief (200ms) doubling of speed occurred (at an unpredictable time). As a secondary benefit, this attention to the adapter also increases the strength of adaptation (Rezec et al., 2004). Trials in which the subjects failed to detect the speed changes were removed from the analysis.

Paradigm 3. Recovery

This paradigm probed the influence of tACS on recovery from adaptation. In this experiment, the time between adapter and test (during which the screen was blank) was 4s; in most subjects this still produces a residual aftereffect (Spigel, 1964). In separate sessions, either no tACS was ever applied, or tACS was applied during each 4s blank period.

Paradigm 4. Pre stimulus tACS

This paradigm investigated whether behavioral effects of tACS require the neural changes induced by adaptation. Each trial started with a 4s blank period, followed by an interval of 500 ms and then by the Test stimulus. In separate sessions, stimulation was either always off or on during every 4s pre-stimulus blank period.

Data Analysis

Curve fitting:

We used Probit Analysis (Finney, 1947) to evaluate the data. We fit the behavioral choice data (proportion of upward choice) with cumulative Gaussians using MATLAB (MathWorks, Natick, MA). We assumed binomial noise on the proportion of up/down responses. The fitted curves all had R^2 values above 0.7. The curve fits provided us with two dependent measures; the point of subjective equality (PSE) and the sensitivity. The PSE was defined as the coherence level at which the fitted curve reached 0.5 and the sensitivity as the slope of the fitted curve at the PSE. We quantified the motion after effect (MAE) as the difference between

the PSE of the adapted and unadapted conditions (both in the absence of tACS) (Hiris and Blake, 1992; Castet et al., 2002).

Statistical Analysis

At the single subject level we used non-parametric permutation tests (Efron and Tibshirani, 1994) to determine whether PSEs and sensitivities were significantly different between two conditions (e.g. adapted without tACS and adapted with tACS). In this procedure we combined the responses from all trials in both conditions, drew (with replacement) two complete datasets from this distribution, and determined the difference in the PSE or sensitivity. We repeated this resampling process 1000 times to obtain a null distribution of the differences. We then determined the p-value of the test as the fraction of values in the null distribution that were larger than the actual difference between the two conditions. Unlike the methods that are derived from asymptotic theory, the bootstrap method is ideal for analyzing psychophysical data because its accuracy does not depend on large numbers of trials, or assumptions (such as normality) about the underlying distributions (Hinkley, 1988).

At the group level, we performed a paired Wilcoxon signed rank test separately for the motion discrimination, motion adaptation, recovery from adaptation, and pre-stimulus tACS experiments. For the motion adaptation and the motion discrimination experiments we also used a two-sided Wilcoxon ranksum test to compare the differences in the changes (sensitivity and PSE) induced by tACS during the contralateral versus the ipsilateral condition. All statistical conclusions

remained the same even after the exclusion of the data collected from the non-naïve subject.

Analysis of the relation between adaptation strength and tACS-induced effects

To investigate whether the influence of tACS (on the PSE or the slope) increased with the strength of adaptation, we calculated the Pearson correlation coefficient (ρ) between the tACS-induced change and the MAE. Specifically, for the change in PSE:

$$\rho = \mathrm{corr}(PSE_{adapt,tACS} - PSE_{adapt}, PSE_{adapt} - PSE_{unadapt}).$$

We used a permutation test to test the null hypothesis that this correlation was larger for contralateral than for ipsilateral tACS stimulation. We created a null distribution of differences in correlation by randomly sampling PSEs from the ipsilateral and contralateral conditions, and calculating the difference in ρ for 1000 shuffled data sets. A statistically significant difference in correlation between contralateral and ipsilateral tACS was defined as a difference in ρ that was larger than the 95th percentile of this null distribution. The analogous analysis was performed for the sensitivity data.

3.4. Results

We measured the influence of tACS (±0.5mA, 10 Hz) on motion sensitivity and adaptation by applying it at various times during a standard motion discrimination

task; during discrimination, before discrimination, during adaptation, and during recovery from adaptation.

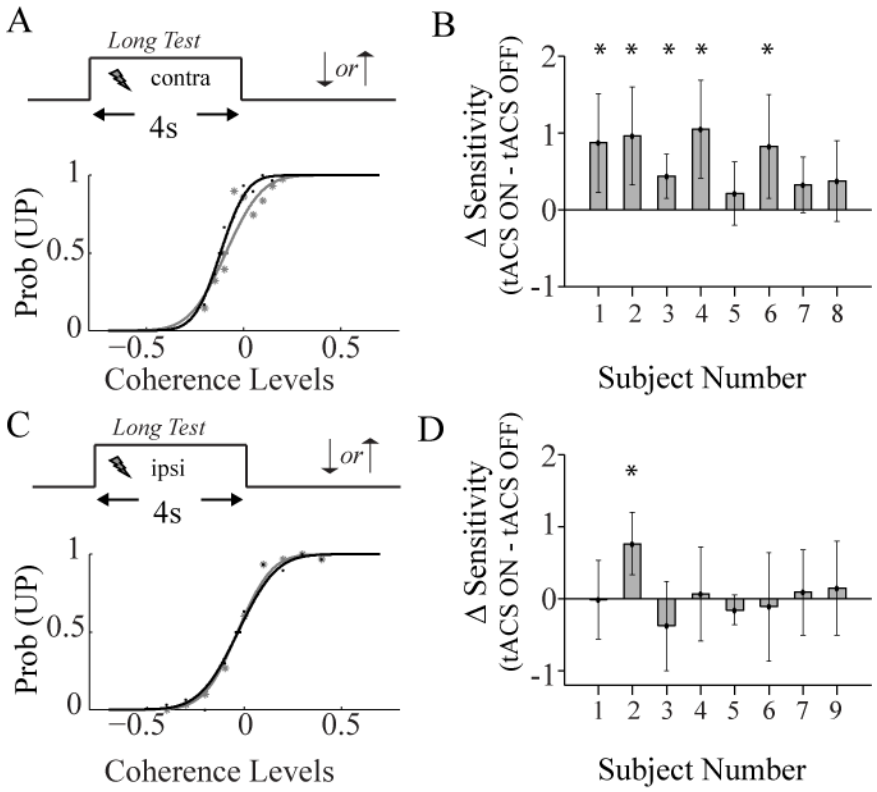

Figure 3.2 Motion Discrimination Task. A. (Top) Task Design. (Bottom) Psychometric functions computed for an example subject with (thick black curve) and without (thin gray curve) tACS. B. Change in sensitivity after application of tACS (for all eight subjects). Error bars indicate bootstrapped standard deviations of the sensitivity estimate. C-D: Same as A-B for the ipsilateral motion discrimination task. * indicates a significant change in sensitivity for an individual subject. These data show that tACS improved motion sensitivity in the contralateral, but not in the ipsilateral hemifield.

tACS improved motion sensitivity

We first tested the hypothesis that tACS injects nuisance perturbations in the motion direction discrimination system. This hypothesis predicts a decrease in the

subjects' sensitivity when tACS is applied over hMT+ during a motion discrimination task. (See Methods; Paradigm 1). Figure 3.2A (bottom) shows the performance of one of the subjects with (thick black curve) and without (thin gray curve) stimulation. From such curves we extracted the two measures of interest; the Point of Subjective Equality (PSE) and the sensitivity (see Methods). Contrary to our expectation, transcranial stimulation improved discrimination sensitivity (Figure 3.2B, $p < 0.05$, Wilcoxon signed rank test; Cohen's $d = 0.79$; effect size $(r) = 0.36$).

The functioning of area hMT+ is lateralized, that is, the right hemisphere responds primarily to stimuli presented in the left visual field and vice versa (Dukelow et al., 2001). This allowed us to perform control experiments to assess the selectivity of tACS and exclude a number of potential confounds. In these experiments the parietal electrode was placed ipsilateral to the visual stimulus. Assuming that the tACS-induced fields are at least coarsely localized (i.e. within a hemisphere), this should not affect motion processing, hence these experiments control for general changes in arousal or attention induced by tACS (see Discussion).

Stimulating the ipsilateral hemisphere did not induce any consistent change in performance (Figure 3.2**C-2D**, $p>0.05$). Moreover, the sensitivity during contralateral stimulation was significantly larger than during ipsilateral stimulation (two sided Wilcoxon ranksum test, $p<0.05$; Cohen's $d = 1.76$; effect size $(r) = 0.66$).

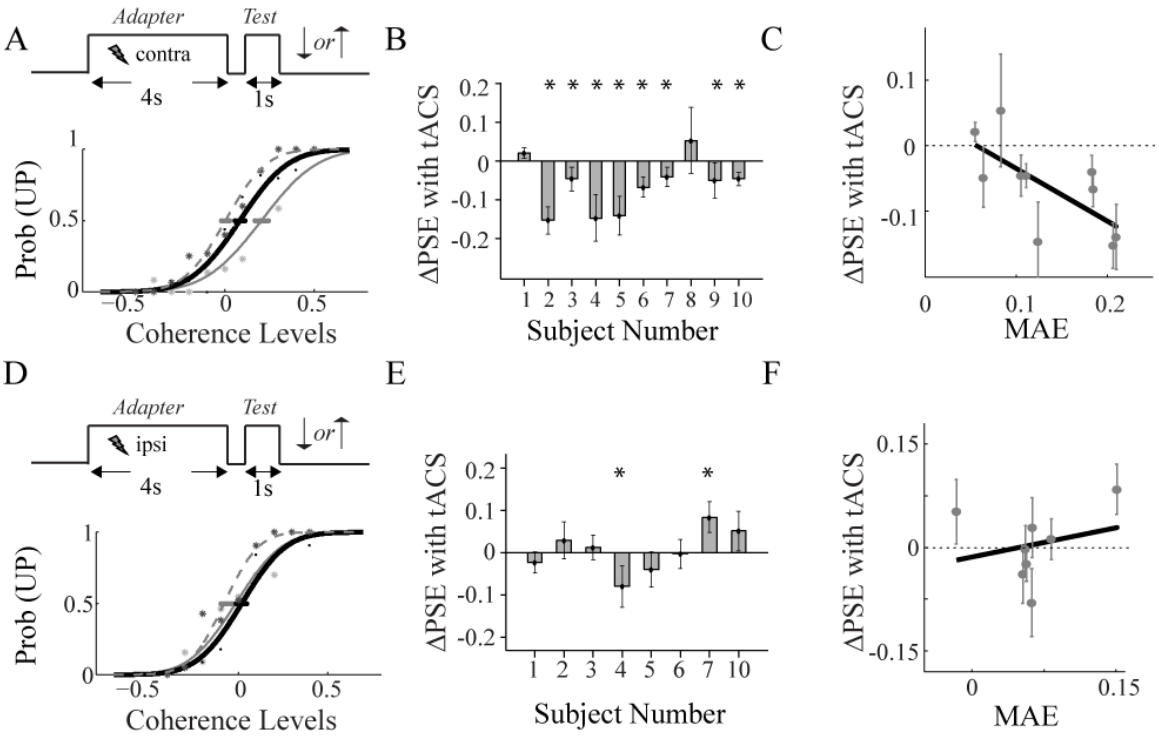

Figure 3.3 Motion Adaptation Task. A. (Top) Task Design for contralateral condition (Bottom) Psychometric functions computed for an example subject with (thick black curve) and without (thin gray curve) tACS. The dashed psychometric curve represents the performance in the unadapted condition. The horizontal error bars refer to the bootstrapped standard deviation of the PSE estimate. B. Change in PSE after application of contralateral tACS (for all ten subjects). Error bars indicate bootstrapped standard deviations of the PSE estimate. C. Changes in PSE with tACS during adaptation (PSEadapt,tACS- PSEadapt) as a function of MAE induced by adaptation without tACS (PSEadapt – PSEunadapt). The black solid line is a linear orthonormal fit to the data points. D-F: Same as A-C but for the ipsilateral condition. * indicates a significant change in PSE for an individual subject. Contralateral but not ipsilateral tACS reduced motion adaptation proportional to the amount of adaptation induced without tACS.

tACS attenuated the motion after effect

In a second set of experiments we tested the hypothesis that tACS affected a form of plasticity that is reflected in the behavioral changes occurring after prolonged exposure to a moving stimulus. Specifically, we determined psychometric curves for motion discrimination before and after motion adaptation, with and without contralateral or ipsilateral tACS during the adaptation phase (See Methods; Paradigm 2).Figure 3.3A (bottom) shows the results for one subject: the dashed curve is the psychometric curve in the unadapted condition. The PSE was at -0.08, which means that this subject reported upward and downward motion equally often when the fraction of downward moving dots was 8% (indicating an upward bias). After adaptation the (thin solid) psychometric curve was shifted rightward to a PSE of +0.13. Hence, after adaptation a pattern in which 13% of the dots moved upward was reported to move upward or downward equally often. This is the MAE, which we quantified as the difference in the PSE between the adapted and unadapted condition (Castet et al., 2002). For this subject the MAE size was PSE_{adapt} - $PSE_{unadapt}$ = 13%- (-8%) = 21%. The thick solid psychometric curve shows the results when tACS was applied during the adaptation phase, this curve is shifted less compared to the unadapted curve, which shows that tACS reduced the MAE. We quantified the tACS effect as the difference in PSE between the stimulated and not-stimulated adaptation condition: $PSE_{adapt,tACS} – PSE_{adapt}$= -2% -13% = -15%.

Across the group of subjects the contralateral application of tACS during motion adaptation significantly reduced the MAE (Figure 3.3A-B; $p<0.05$, Wilcoxon signed rank test; Cohen's d = 0.93, effect size(r) = 0.42). By comparison, ipsilateral

stimulation did not yield a significant change in MAE (Figure 3.3D-E; $p>0.05$), and a direct comparison showed that the effect of contralateral tACS was significantly larger than ipsilateral tACS ($p<0.05$; Cohen's $d = 0.90$, effect size (r) = 0.41).

Subjects with a large MAE in the absence of tACS typically had a larger reduction in MAE when tACS was applied (Figure 3.3C). This negative correlation supports the idea that tACS interferes with the mechanisms of adaptation (Figure 3.3C; Pearson correlation coefficient = -0.63). Such a correlation was not found for ipsilateral stimulation (Figure 3.3F), and a permutation test (see Methods) confirmed that the correlation induced by contralateral stimulation was significantly larger than that induced by ipsilateral tACS.

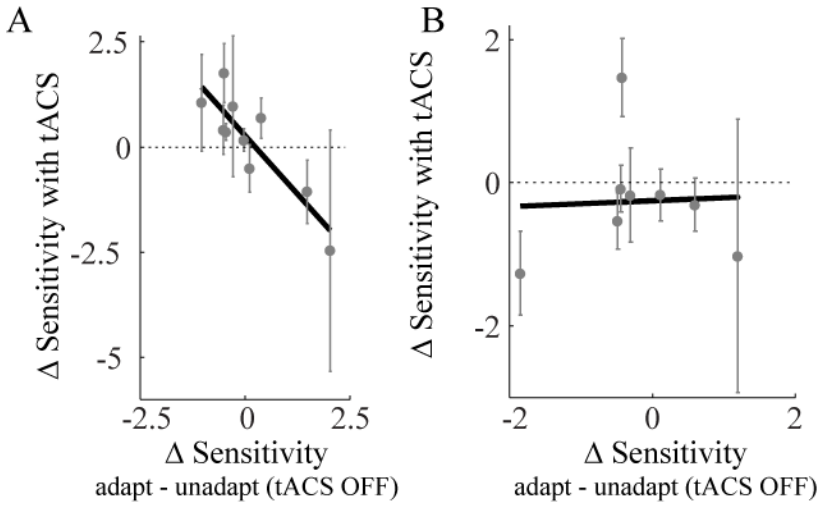

Figure 3.4 Sensitivity changes during motion adaptation. A. Changes in sensitivity with contralateral tACS during adaptation ($Sensitivity_{adapt,tACS}$-$Sensitivity_{adapt}$) as a function of sensitivity changes induced by adaptation without tACS ($Sensitivity_{adapt}$-$Sensitivity_{unadapt}$). B. Changes in sensitivity with ipsilateral tACS. The black solid lines are linear orthonormal fits to the data points. Sensitivity changes induced by adaptation were attenuated by contralateral tACS, but unaffected by ipsilateral tACS.

tACS attenuated sensitivity changes during adaptation

Adaptation not only shifted the psychometric curve, it also changed its slope, a measure of subjects' sensitivity to motion. This is consistent with the results of Van Wezel and Britten (2002), who demonstrated that adaptation reduces motion sensitivity. We found a similar reduction in sensitivity (a shallower slope) in most of our subjects. For each of those subjects, tACS increased sensitivity. For two of our subjects adaptation significantly increased sensitivity; for those subjects tACS decreased sensitivity. This negative correlation is further evidence that tACS attenuates adaptation (Figure 3.4A, Pearson correlation is -0.68). This relationship was not found during ipsilateral stimulation (Figure 3.4B) and the difference between the contralateral and ipsilateral condition was statistically significant (permutation test; $p<0.05$; see Methods).

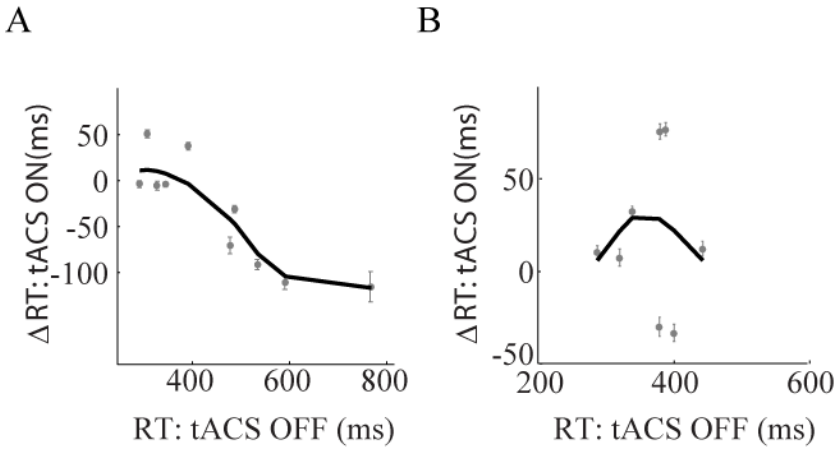

Figure 3.5 Reaction time (RT) changes during tACS. **A.** Changes in reaction time (ΔRT) in the speed detection task induced by tACS as a function of reaction times without tACS. The bold line is a robust locally weighted polynomial regression fit to the data. The vertical error bars represent the standard error. **B.** Same as A, now for ipsilateral stimulation. tACS reduced reaction times, but only for contralateral visual stimuli.

To control and monitor the allocation of attention, the subjects performed a speed detection task during the adaptation phase. This provided us with an additional and independent measure of motion sensitivity. We found that contralateral stimulation reduced subjects' reaction time on this task (Figure 3.5A). This was mainly driven by subjects whose reaction times were long in the absence of tACS. Ipsilateral stimulation, on the other hand, did not affect the reaction time systematically (Figure 3.5B).

tACS did not affect recovery from adaptation

In our adaptation paradigm, we can distinguish between an induction phase (the time when the adapter was on the screen) and a recovery phase (defined here as the time between the adapter and the test stimulus, when the screen was blank). The previous experiment showed that tACS during the induction phase reduced the MAE. Here we investigated whether tACS during recovery could also change the MAE.

We increased the duration of the recovery phase (the time between adapter and test) to 4s, and applied tACS only during recovery. In this phase, the subjects had already been adapted to the prior visual stimuli (Top-up Adapter) but they did not receive visual motion input (See Methods; Paradigm 3). Stimulation in the recovery phase had no significant effect on the subsequent MAE nor did it change the slope of the psychometric curves ($p>0.05$; average $\Delta PSE = 0.01$, s.d =0.05), average

ΔSensitivity =-0.0067, s.d = 0.82). In other words, tACS affected the induction of adaptation (Figure 3.3), but not the recovery from adaptation.

tACS effects required motion adaptation

In the motion adaptation experiments above, tACS was always applied well before the test stimulus (together with the adapter), hence it is possible that simply preceding a test stimulus by tACS induced a behavioral effect and that adaptation was not required per-sé. To test this hypothesis, we performed experiments in which each test stimulus was preceded by 4s of a blank screen. tACS was applied only during this blank period (See Methods; paradigm 4). Under these conditions, there was no significant effect of tACS on the PSE or sensitivity ($p>0.05$; average ΔPSE = 0.02, s.d = 0.06, average ΔSensitivity = -0.19, s.d = 1.33). In other words, when applied outside the adaptation context, tACS had no effect, supporting our interpretation that tACS interfered with adaptation.

3.5. Discussion

We investigated how transcranial alternating currents affect human motion perception. We found that tACS reduced motion adaptation and improved motion discrimination sensitivity. Electrical stimulation did not affect motion perception when applied before visual stimulus presentation, or during the recovery phase of adaptation. Taken together, these findings can be summarized succinctly as demonstrating that tACS attenuates the induction of adaptation.

We first address some of the confounding factors and limitations in the interpretation of our data. Then we speculate on the neural mechanisms that could be involved in this and conclude with a brief discussion of the implications of our findings for the practical usage of tACS.

Confounds

Transcranial AC stimulation at 10Hz can generate phosphenes due to current spread to the retina (Kar and Krekelberg, 2012). As an additional "visual" stimulus that is only present in the tACS conditions, these retinal phosphenes could in principle interfere with adaptation. Several arguments, however, speak against this. First, phosphenes occur in the periphery (Kar and Krekelberg, 2012) and - given the receptive field locations (Hartmann et al., 2011) of neurons in motion areas - the visual stimulation induced by tACS phosphenes and the motion stimulus affect non-overlapping populations of neurons. Second, tACS induces phosphenes in both hemifields, with no obvious patterns of lateralization (Kar and Krekelberg, 2012). Hence if tACS reduced adaptation by drawing attention away from the adapter (Chaudhuri, 1990) one would expect to find it in both ipsilateral and contralateral stimulation conditions. Our control experiment (Figure 3.3D), however, shows that only contralateral stimulation reduced adaptation. The specificity of the effect for contralateral tACS also argues that the action of tACS is significantly more pronounced in the cortical hemisphere over which it is applied and is incompatible with a general change in arousal induced directly or indirectly via the generation of phosphenes.

Limitations

The amplitude of tACS in our experiments was 0.5 mA, and its temporal frequency was 10 Hz. Of course many other patterns of stimulation are possible (different frequencies, or non-sinusoidal patterns, different electrode montages) and potentially worth exploring. We note, however, that this is an extremely large search space, and more insight into the underlying mechanisms may be required to perform an informed search.

Under our particular experimental conditions, we found that tACS increased motion sensitivity. This is incompatible with the view that tACS injects neural noise or perturbations. Of course, one cannot extrapolate such a finding to higher currents, other temporal frequencies, or other stimulation patterns. In fact it is inevitably the case that at high enough currents, tACS would impact behavioral performance negatively and therefore be behaviorally equivalent to the injection of “noise”.

Comparison with tDCS

Antal et al. (2004) have shown that transcranial direct current stimulation (tDCS) over hMT+ reduces the subjective duration of the motion after effect. The goal of the Antal et al. (2004) study, however, was not to investigate which aspects of motion adaptation tDCS interferes with, but to provide support for the causal involvement of hMT+ in the MAE. Presumably for this reason, tDCS was applied continuously both during adaptation induction, recovery, and the subsequent motion detection task. Hence, the reduction in MAE duration could have been the consequence of tDCS’ interference with any of these processes; this prevents a

direct comparison with our findings. Nevertheless, it is of interest to note that Antal and colleagues found that tDCS reduced the MAE irrespective of whether the anode or the cathode was placed over hMT+. This is compatible with our finding that tACS, which also generates current flow of both polarities, attenuates adaptation. Our behavioral data cannot address the question whether the same mechanisms underlie the influence of tACS and tDCS, but for tDCS we can speculate that the underlying mechanism is likely different from the (polarity dependent) modulation of excitability reported in motor cortex (Nitsche et al., 2005).

Mechanism

Our experiments show that tACS attenuates motion adaptation. Hence, one would expect that tACS attenuates any of the consequences of adaptation. Together with the finding that motion adaptation reduces performance on a coarse motion detection task (Van Wezel and Britten, 2002) this provides a succinct explanation of the behavioral changes we observed. For instance, tACS increased sensitivity and reduced reaction times most for those subjects who showed a large adaptation effect (Figure 3.4A and Figure 3.5A). Importantly, this also accounts for the tACS-induced increase in sensitivity during the presentation of a single RDK (Figure 3.2B). Even though this experiment did not involve a separate adaptation stimulus, the 4 second long RDK likely triggered adaptation. Our data support the view that this adaptation was attenuated by tACS, and this led to an increase in sensitivity.

At the circuit level, prolonged exposure to moving stimuli is known to result in firing rate changes throughout visual cortex. Individual neurons can increase or decrease their firing rate with adaptation and this depends critically on the relationship between the tuning of the neuron and the properties of the adapter and test stimuli. For instance, the speed of the moving stimulus (Krekelberg et al., 2006b), the direction of motion (Kohn and Movshon, 2004), as well as its size and duration (Wissig and Kohn, 2012; Duijnhouwer et al., 2013; Patterson et al., 2013) all affect firing rate changes induced in an adaptation protocol (Krekelberg et al., 2006a). This shows that the consequences of adaptation depend critically on the circuit in which neurons are embedded (Richert et al., 2013) and implies that the consequences of tACS for a single neuron will also depend strongly on its connections within the local circuit. In other words, based on our behavioral observations and the known properties of adaptation at the single neuron level, it seems unlikely that tACS would generally increase or decrease firing in a population of neurons. We plan to test this in the future using extracellular recording in the middle temporal area of the macaque during transcranial stimulation.

Linking behavioral data with cellular mechanisms requires many assumptions, and is inevitably speculative. Nevertheless, we believe it is valuable to put forward a novel and testable hypothesis that aims to do so. We start from the observation that small membrane voltage fluctuations reduce spike frequency adaptation, as shown by in-vitro recordings of rat hippocampal CA1 neurons using direct somatic current injection (Fernandez et al., 2011). We speculate that tACS could induce

such membrane fluctuations in the soma or dendrites and thereby interfere with adaptation.

Two major questions need to be answered before this can be accepted as a viable mechanism. First, can tACS generate membrane fluctuations that are large enough? Current finite element current flow models predict membrane voltage changes at pyramidal cell somas on the order of 0.2 mV (Radman et al., 2009; Reato et al., 2013). While it should be noted that considerable uncertainty is associated with these predictions, this is an order of magnitude smaller than the somatic voltage fluctuations (~2 mV) used by Fernandez et al. (2011). Second, do small membrane fluctuations generate effects that last long enough? Fernandez et al. (2011) argue that voltage fluctuations reduce spike frequency adaptation through Na^+ de-inactivation. Given the rapid time course of de-inactivation, this mechanism alone is unlikely to lead to behavioral effects that last several seconds. Slice recordings could address these questions. The first by measuring whether smaller somatic voltage fluctuations suffice to reduce adaptation, or by investigating the role of dendritic voltage fluctuations. The second by determining whether the slower voltage or Na^+ dependent K-channels known to be involved in adaptation (Sanchez-Vives et al., 2000a), are also affected by membrane fluctuations.

Implications for tACS usage

Current understanding of direct current stimulation (tDCS) is that the orientation of a neuron in the applied field determines whether its excitability will be increased or decreased through a net depolarization or hyperpolarization of the soma (Radman

et al., 2009). If, however, tACS influences neurons through the interaction of sub threshold oscillations with adaptation, then it would be affected less by the orientation of the neuron in the field. Given that field orientation in a target area is highly idiosyncratic and difficult to predict (Datta et al., 2009), this could be a considerable practical advantage of tACS over tDCS.

CHAPTER 4

Comparison between effects of transcranial direct current and alternating current stimulation during visual motion discrimination

In chapter 3, I provided empirical evidence for the role of 10 Hz tACS in attenuating motion adaptation. Although I provide a strong case for the anti-adaptation effects of tACS, there remain a lot of unanswered questions. First, are the behavioral effects dependent on the frequency of tACS? Second, would tDCS applied for the same duration result in similar effects? Third, do the behavioral effects of tACS outlast its application time? In the study presented in this chapter, I have explicitly tried to answer these questions. This chapter is a manuscript in preparation for publication.

4.1. Abstract

Transcranial current (direct current and alternating current) stimulation (tCS) has been demonstrated as a potential noninvasive neuromodulatory tool. The effects of tCS range from cognitive enhancements to clinical benefits. Although both DC and AC transcranial stimulation has been shown to produce behavioral modulation, a direct comparison of the two during an identical task is lacking. We also have limited knowledge about the time course of tACS induced behavioral effects; specifically whether it outlasts the application time. In addition, whether tACS can modify behavior in a frequency dependent manner is of importance given the varied role of different brain oscillations in human behavior. We have recently demonstrated that when 10Hz tACS is applied simultaneously during a coarse motion direction discrimination task over the parietal cortex, it improves subject's discrimination sensitivity. Here we specifically contrasted the effects of multiple tACS frequencies with short term anodal and cathodal tDCS during motion discrimination. We have three primary findings. First, short-term tDCS doesn't provide performance enhancement during motion discrimination. Second, tACS improves discrimination sensitivities for multiple frequencies and the effect is limited to the contralateral hemifield. However, we observed a marginal deterioration of performance at the beta frequency (20 Hz). Third, the effects of tACS outlast its application time. Our results highlight the advantage of tACS over tDCS for short term enhancement in performance.

4.2. Introduction

Both transcranial direct current (tDCS) and alternating current (tACS) stimulation have been established as promising neuromodulatory tools for noninvasive brain stimulation (Brunoni et al., 2012; Herrmann et al., 2013). Despite the widespread use of these two techniques (Reppas and Newsome, 2007), we know very little about the underlying mechanisms and the differences between them. This prevents clinicians and basic science researchers from choosing the optimal technique for any given task.

The commonly accepted mechanism of tDCS is that it produces subthreshold membrane polarization (Priori et al., 1998). The long lasting after-effects of tDCS (Nitsche and Paulus, 2001) are mediated by NMDA glutamatergic receptor dependent changes (Nitsche et al., 2003). In addition, a number of reports suggest that anodal tDCS (atDCS) increases excitability whereas cathodal tDCS (ctDCS) decreases it (Nitsche and Paulus, 2000). Most tDCS protocols involve 10 or more minutes of stimulation time with pronounced behavioral effects lasting over an hour (for review see Nitsche et al., 2008). However, short term application of low intensity tDCS (<0.5 mA, 7s) on the motor cortex (Priori et al., 1998) can also produce changes in motor evoked potentials (MEP). On the other hand, fewer studies have investigated the effects of tACS while varying the parameters of stimulation. One of the first study to compare tACS and tDCS effects (2 to 10 minutes of stimulation) on the motor cortex reported no significant changes in MEP with tACS. Here we specifically compared short term tDCS with tACS during a coarse motion discrimination task.

Different brain oscillations have been implicated in different brain functions (Basar et al., 2001). In the human visual cortex, the role of alpha (8-12 Hz) oscillations has been controversial. Traditionally, alpha waves have been associated with lack of sensory stimulation (Pfurtscheller et al., 1996). But recent studies show that both amplitude and phase of alpha frequencies are modulated by attention and visual perception (de Graaf et al., 2013). Similarly, synchronized beta (15-30 Hz) oscillations has been implicated in perceptual rivalry (Piantoni et al., 2010). Stimulus driven gamma (30-80 Hz) oscillations have also been observed in human ECoG data (Hermes et al., 2014). Taken together, these facts make the visual cortex a promising area to test the effects of different tACS frequencies.

We have previously shown that 10 Hz tACS over human parietal cortex improves coarse motion discrimination (Kar and Krekelberg, 2014). The human motion detection system has been relatively well explored (Huk et al., 2001) and the mechanistic predictions from the behavioral results can be electro-physiologically tested in homologous macaque brain areas (Orban et al., 2003). Hence, in two sets of experiments, we extended our previous paradigm to test the effects of multiple tACS frequencies and also short term tDCS, respectively. We also estimated the time course of tACS induced effects.

We observed that contralateral application of tACS improves motion discrimination in a frequency independent manner and the effects outlast the application time. On the other hand, we did not find any significant effect of tDCS on motion discrimination.

4.3. Materials and Methods

Subjects

Thirteen subjects participated in the experiments (seven female).They gave written consent and had normal or corrected to normal vision. This study was conducted according to the principles expressed in the Declaration of Helsinki and approved by the Institutional Review Board of Rutgers University.

Experimental Procedures

Subjects were seated in a dark room at a distance of 57cm from the center of the monitor. Head movements were restricted by a molded bite bar. The subjects indicated their response using the keyboard. Fixation of a central red dot was monitored and trials in which the eye strayed beyond a virtual window of 2^{o} degree were discarded.

Apparatus

tACS was delivered through a STG4002 stimulus generator (Multi Channel Systems, Reutlingen, Germany). The stimulating electrodes were prepared as saline soaked sponges attached to conductive rubber electrodes (3" diameter). We either used a rectangular pulse of ±0.5 mA or sinusoidal currents (1 mA peak to peak) at a frequencies of 5, 10, 20, 30, 50 and 80 Hz. For safety reasons, the maximum voltage to produce the transcranial current was limited to 20V. The maximum current density was 0.01 mA/cm^2 (current intensity = 0.5 mA; electrode surface area = 45.6cm^2). All eye movements were recorded using an eye tracker

(Eyelink II V 2.2) at 500 Hz. All events in a trial were synchronized and triggered using in house software Neurostim (http://neurostim.sourceforge.net).

Electrode Placement

One electrode was placed above the canonical location of left hMT+; PO7-PO3 in the 10-20 system. The other electrode was placed on the vertex. With the exception of the ipsilateral control experiments (below), the parietal electrode was always contralateral to the visual stimuli.

Visual Stimuli

Stimuli were presented on a CRT monitor (Sony FD Trinitron) with a resolution of 1024 x 768 pixels at a refresh rate of 120 Hz. The main motion stimulus was a dynamic random dot kinematogram (RDK) consisting of 700 dots (1.5 pixels in diameter) with infinite lifetime. The dots were restricted inside a circular aperture of radius 5^o centered 7^o to the left or right of the center of the screen. The luminance of the dots was 30 cd/m^2, the background 0.4 cd/m^2. The dots moved at a constant speed of 3 ^{o}/s. We refer to the percentage of dots moving in the same direction (up or down) as the coherence. The remainder of the dots moved in randomly chosen directions.

Motion discrimination task

This paradigm served to measure the instantaneous influence of tACS and short term tDCS (both polarities) on coarse motion discrimination. In each trial, we presented a RDK (*Test* stimulus) with different levels of coherence and the subjects indicated the perceived global direction of motion (up or down). The coherence of the stimuli ranged from -100% (all dots moving down) to +100% (all

dots moving up). Stimulation was applied over the left hMT+ during the visual stimuli (Figure 4.1).

tDCS protocol. In separate sessions, the visual stimulus was either presented in the right hemifield (contralateral condition) or left hemifield (ipsilateral condition) with or without short term tDCS. We refer to the placement of the positive electrode over PO7-PO3 and negative over the vertex as the anodal tDCS (atDCS) condition and the opposite as cathodal tDCS (ctDCS) condition.

tACS protocol. We interleaved trials with different tACS frequencies (at 5, 10, 20, 30, 50 and 80 Hz) and no stimulation. We conducted the contralateral and ipsilateral conditions in separate sessions.

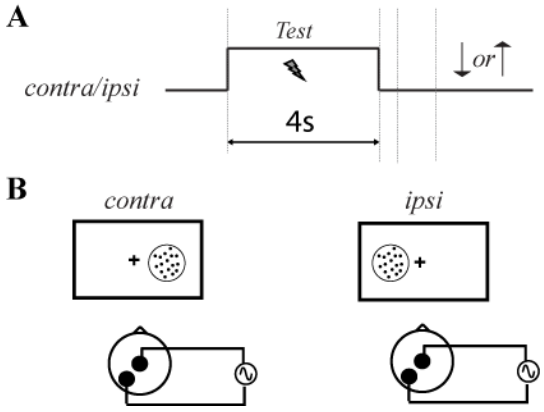

Figure 4.1 Design of the behavioral task. A) Experimental paradigm. In each trial we presented a random motion dot stimuli (*Test*) at varying degree of coherence (up or down). The subject's task was to respond 'UP' (↑) or 'DOWN' (↓) depending on the coherence of the stimuli. tDCS or tACS (↯) was applied simultaneously during the presentation of the *Test* stimuli, in the respective conditions. B) Stimulation was applied over the left hMT+. The visual stimuli was presented either on the contralateral or the ipsilateral hemifield in separate sessions.

Data Analysis

Psychometric function estimates before accounting for history dependent effects

We first separated all trials with unique conditions (no stimulation, atDCS, ctDCS, and tACS with 5, 10, 20, 30, 50 and 80 Hz). We analyzed each condition independently for each subject. We used Probit Analysis (Finney, 1947) to evaluate the data. We fitted the behavioral data (variation of proportion of upward choice with coherence) with cumulative Gaussians using MATLAB (MathWorks, Natick, MA). We assumed binomial noise on the proportion of up/down responses. The curve fits provided us with two dependent measures; the point of subjective

equality (PSE) and the sensitivity. The PSE was defined as the coherence level at which the fitted curve reached 0.5 and the sensitivity as the slope of the fitted curve at the PSE.

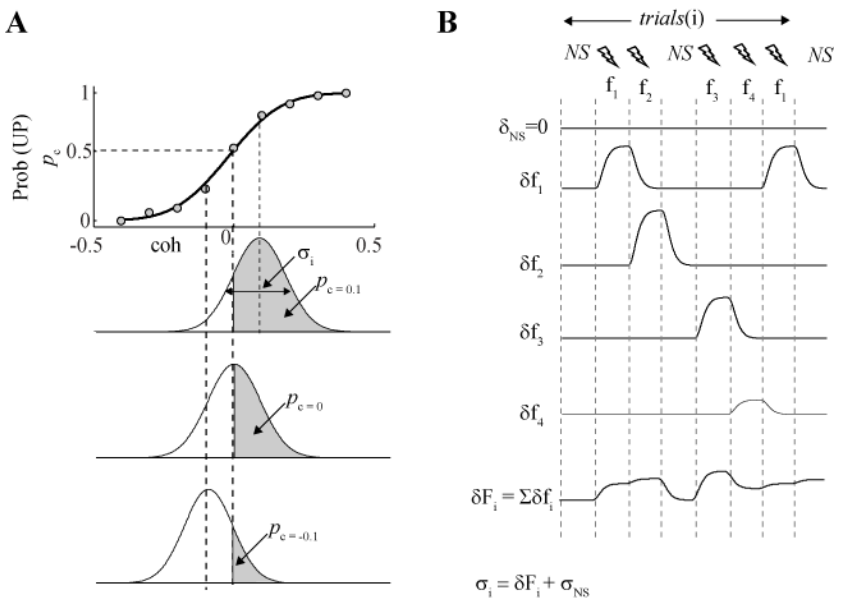

Figure 4.2 Computational model to account for long term effects of tACS. A) Motion discrimination model. The top panel shows performance of an ideal subject in the motion discrimination task. Coherence is shown in the abscissa and probability of choosing 'UP', Prob (UP) for each coherence (p_c) is plotted in the ordinate. The black curve is the cumulative Gaussian fit (psychometric function) for the data. The three bottom panels show how the model estimates Prob (UP), area under the curve from 0 to $\propto$ (gray shade) for each coherence, given a specific variance (σ) in performance. B) Demonstration of how the long term effects of each tACS trial is incorporated in the analysis. The time course of the change in variance induced by a specific tACS frequency (δf) is taken into account for each trial.

Psychometric function estimates after accounting for history dependent effects

We model each trial *i* of an experiment as an independent Bernoulli trial. The probability p_i of choosing upward motion on the i^{th} trial is dependent on the coherence c_i of the dot motion and subject's internal noise variance σ_i for that trial.

$p_i = 1 - \text{normcdf}(0, c_i, \sigma_i)$,

where normcdf(0, c_i, σ_i) returns the normal cumulative distribution function at the value 0 using the specific values for the mean c_i and standard deviation σ_i.

The model assumes that for each trial, the binary response r_i (0: downward and 1: upward) is a single draw from a binomial distribution with a probability p_i .

The time varying effects of tACS (δ_f) at a frequency *f* on the subject's internal variance without stimulation σ_{no_stim} is modeled as a temporal impulse response function. The temporal impulse response function, at each time point t from tACS onset is modelled as a gamma probability distribution function (gampdf) with two parameters α (shape) and β (scale)

$\delta_f(t) = A_f * \text{gampdf}(t,\alpha,\beta)$, where A_f is the maximum magnitude of the function at frequency f and t is the time from tACS onset.

Since this function can be non-zero at the time of tACS offset, the model accounts for long lasting changes induced by tACS. At any given trial (i), the subject's internal variance σ_i is a sum of the subject's internal variance without stimulation σ_{no_stim} and the resultant δ (accounting for all previous trials and the current trial).

So at the end of an experiment we have a response vector R = (r_1, r_2, . . ., r_n) which represents the outcomes of *n* independent Bernoulli trials, each with success probability p_i .

The likelihood for p_i based on *R* is defined as the joint probability distribution of r_1, r_2, . . . , r_n.

$L(\theta;r) = \prod_{i=1}^{n} p_i^{r_i} * (1 - p_i)^{(1-r_i)}$

In our model we have a set of parameters $\theta = (A_f, \alpha, \beta, \sigma_{no\_stim})$. Given a set of these parameter values, we can generate the p_i for each trial of an experiment. We estimate the parameters of the model by minimizing the negative log-likelihood of the function L(θ;R) where R is the set of responses for the trials from a human subject under different conditions.

Statistical Analyses

We assessed the effects of transcranial current stimulation on the internal variance with a two-way repeated-measures ANOVA. The first factor was stimulation type, tDCS (cathodal and anodal) or tACS (5, 10, 20, 30, 50 and 80 Hz). The second factor was visual hemifield (ipsilateral and contralateral).

4.4. Results

We measured the changes in human subjects' performance under the concurrent application of short term (four seconds) anodal and cathodal tDCS and tACS at multiple frequencies (5, 10, 20, 30, 50, and 80 Hz) during a coarse motion direction

discrimination task. We also estimated the long lasting effects of tACS on the subjects' performance.

Short term tDCS for either polarity do not improve motion sensitivity

We first investigated whether short term application of tDCS of either polarity (cathodal and anodal) had any effect on coarse motion direction discrimination. Previous studies have shown that tDCS effects reverses based on the polarity (Nitsche et al., 2002). Hence we hypothesized that tDCS will induce a polarity dependent change in subject's performance. Figure 4.3A shows the comparison of effects of atDCS and ctDCS applied during the contralateral and ipsilateral conditions respectively. We found no significant changes ($p>0.05$) in discrimination sensitivity on application of tDCS.

tACS improved sensitivity during contralateral stimulation

We have previously shown that 10 Hz tACS improves motion discrimination sensitivity when applied concurrently during the task (Kar and Krekelberg, 2014). Here we tested how the effects depend on the tACS frequencies. We used a randomly interleaved trial structure to apply multiple tACS frequencies along with trials with no tACS. Figure 4.3B shows the comparison of effects during contralateral and ipsilateral conditions, when the data was analyzed assuming no long lasting effects of tACS. We observe no significant changes between the two

conditions under this assumption. To test whether the application of any tACS frequency in a trial had an effect that outlasted its application time and affected subsequent trials we compared the estimated discrimination sensitivities between non-stimulated trials which were either preceded by a non-stimulated trial and a stimulated trial. Figure 4.3C shows the comparison of all non-stimulation trials preceded by non-stimulation trials (gray curve) to all non-stimulation trials preceded by 5Hz tACS (black curve). The inset shows that the discrimination sensitivities were significantly different (permutation test; $p<0.05$). Hence we conclude that tACS application has long lasting effects and we need to account for that in order to accurately estimate the changes in parameters. Figure 4.3D shows that after accounting for the long lasting effects of tACS (refer Methods), we do observe that contralateral tACS improves motion discrimination significantly ($F = 5.18$, $p < 0.05$). We did not find any effect of the factor frequency in the ANOVA. However 20 Hz tACS showed a significant different effect on subject's performance than the rest of the applied tACS frequencies. Figure 4.3E shows that 20 Hz tACS significantly deteriorated the subjects' performance.

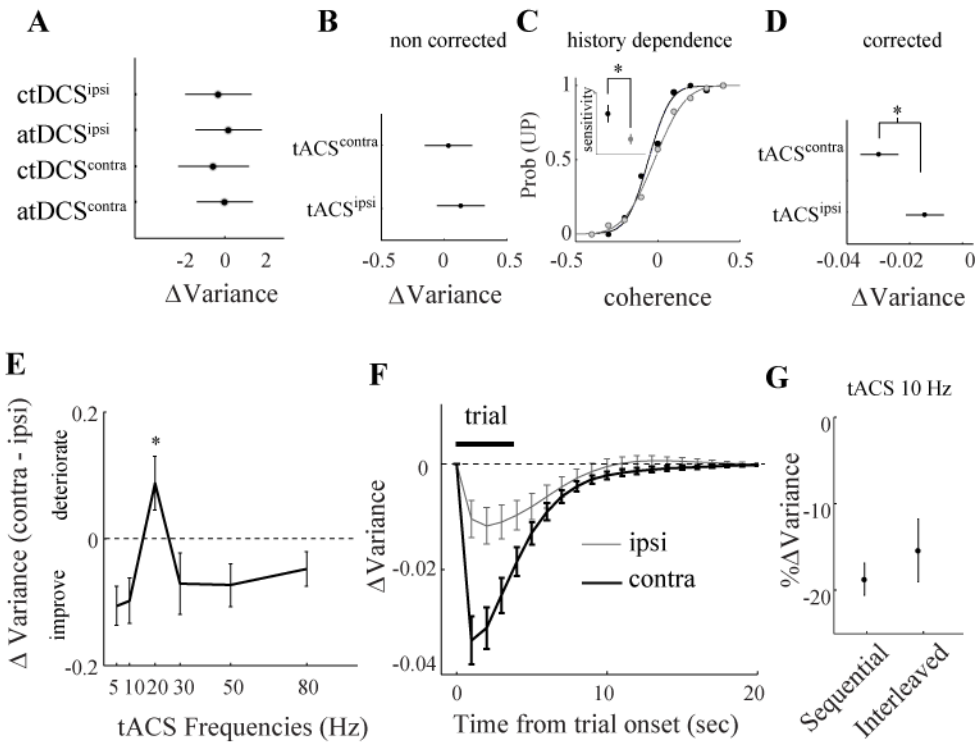

Figure 4.3 Effects of tDCS and tACS on motion discrimination. A) Change in variance with anodal and cathodal tDCS for both ipsilateral and contralateral stimulation. There is no significant change in variance with tDCS B) Effects of tACS (averaged across all frequencies) on the variance, without correcting for long term effects of tACS. C) Example of history dependence of tACS effects. Two psychometric functions computed from all non-stimulation trials preceded by non-stimulation trials (gray curve) and all non-stimulation trials preceded by 5Hz tACS trials (black curve) are plotted. The inset shows that the discrimination sensitivities were significantly different. D) Effects of tACS (averaged across all frequencies) on the variance, after correcting for long term effects of tACS. tACS significantly improves motion discrimination. E) Frequency dependence of tACS effects. Apart from a deterioration at 20 Hz, all tACS frequencies tested (5, 10, 30, 50, and 80) showed an improvement. F) Time course of tACS induced effects (gray: ipsilateral condition, black: contralateral condition) for an application time of 4s. G) Comparison of 10 Hz tACS induced sensitivity changes estimated with random presentation of trials (all tACS frequencies interleaved) and sequential presentation of trials (Kar and Krekelberg, 2014). The estimates are not significantly different from each other.

tACS effects outlast the application time

We estimated how long the effect of any tACS frequency applied for 4 seconds lasted after tACS onset. Figure 4.3F shows a comparison of 10 Hz tACS applied during the contralateral (black curve) and ipsilateral (gray curve) respectively. Contralateral stimulation significantly reduce subjects' variance and the effects outlast the stimulation application time. We also notice that ipsilateral stimulation reduces variance (much less than the contralateral condition). We speculate that, this can be induced by overall increased attention due to tACS-induced phosphenes or tactile sensations.

4.5. Discussion

We compared how short term tDCS (cathodal and anodal) and tACS applied at multiple frequencies affect human performance in a coarse motion discrimination task. We found that tACS improved motion discrimination sensitivity in a hemisphere specific manner. We did not observe significant frequency tuning of the effects. We estimated the time course of tACS induced effects. The most parsimonious model for our data predicts that the effect of tACS outlasts the application time. When we applied tDCS for the same duration of time it did not produce any significant performance enhancement.

We first address some of the confounding factors and limitations in the interpretation of frequency tuning of behavioral effects during tACS. Then we

provide a brief speculation on the mechanisms that could account for our results. Finally we conclude with a discussion on some advantages of tACS over tDCS.

Frequency Tuning of tACS

It has been recently shown that tACS at alpha frequency can entrain human EEG activity and modulate behavioral performance (Helfrich et al., 2014). In addition, gamma tACS has also been shown to modulate awareness during sleep (Voss et al., 2014). If we could use specific tACS frequencies to modulate specific brain functions, it would make tACS an extremely versatile tool. Recently, the issue of frequency dependence of tACS has been studied and much debated (Kanai et al., 2008; Kar and Krekelberg, 2012; Turi et al., 2013). Although the possibility of stimulating at different frequencies provide a very interesting dimension for investigation, drawing inference from these behavioral results is confounded by several factors. First, electrical properties of the skull have their own frequency tuning (Akhtari et al., 2002). Second, tACS induces peripheral phosphenes (Kar and Krekelberg, 2012). The phosphene intensities have a temporal frequency tuning and likely drive attentional modulation differentially. Third, the power spectrum of the local field potentials and EEG recordings from humans and macaques show a 1/f distribution (Buzsaki et al., 2012). This might introduce an inherent frequency preference. All these factors can interact nonlinearly to produce the final behavioral outcome. Hence, caution must be exercised before interpreting any frequency dependence of tACS. We observed that at 20 Hz, the subjects' performance was significantly poorer (contralateral compared to ipsilateral,

Figure 4.3E) than that compared to other frequencies. This tuning can purely be a result of differential phosphene intensities across tACS frequencies, which under similar luminance conditions also peaks around 20 Hz (Kanai et al., 2008).

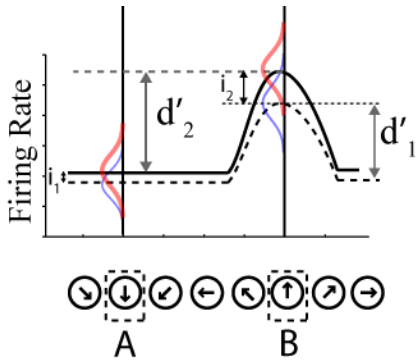

Figure 4.4 Speculated mechanism of tACS. Predicted population response of hMT+ neurons during the presentation of a 70% upward coherent Test stimulus without tACS (dashed curve) and with tACS (bold curve). The red and blue Gaussians represent the variability of the spike rate. d' (difference between the mean activity of the neurons A and B) is a measure of the sensitivity of the system for the task. i_1 and i_2 are the increments in the firing rate due to the mitigation of adaptation induced by tACS.

Putative mechanisms of tACS

Our experiments show that tACS at multiple frequencies improves sensitivity during coarse motion discrimination. Although we only recorded behavioral data, we speculate about the underlying neuronal mechanisms with a qualitative neural population model. Decision making during motion direction discrimination has been previously modelled from population activity of MT neurons (Furman and Wang, 2008). We will use a simple "winner take all" decision model to speculate about ways in which discrimination sensitivity can be improved under application

of tACS. Figure 4.4 provides a cartoon depiction of the population activity profile of a motion direction selective pool of neurons during the presentation of a 70% coherent upward moving RDK stimulus. Given that for this stimulus, the neurons that prefer upward motion (B) are receiving a stronger input than the rest of the neurons, we will likely observe a higher firing rate for those neurons. The dotted gray curve shows the predicted neural responses under no stimulation. We assume that the decision of up versus down is determined by comparing the firing rates of the neurons that prefer upward motion (B) to the firing rates of the neurons that prefer downward motion (A). The Gaussian curves shows the variability of the firing rates at this particular coherence for A and B. The difference in the mean of the Gaussian curves for A and B (d_1) is proportional to the discrimination sensitivity of the subject. Hence this model predicts that the discrimination sensitivity can be improved by increasing the difference between the two Gaussians at A and B. We have previously reported that tACS applied at 10 Hz attenuates motion after effect and mitigates motion-adaptation induced sensitivity changes (Kar and Krekelberg, 2014). We speculate that application of tACS reduces adaptation, thereby increasing the responsivity of the neurons. Since neurons A and B have different input drives, the tACS -induced increase in responsiveness in A (i_1) should be less than that in B (i_2). This leads to the increase in the difference between the two Gaussians (d_2), thereby improving the subject's discrimination sensitivity.

Electrophysiological properties of neurons are sensitive to very weak electric fields (Francis et al., 2003). The effects of these electric fields are amplified due to neuronal network interaction. What specific mechanisms underlie the tACS-

induced changes in responsivity and attenuation of adaptation remains to be answered. We propose two different theoretical approaches towards finding an answer to this question. First, tACS stimulation might lead to a stimulus dependent increase in overall responsivity of all affected neurons. Previous studies using tDCS (Fritsch et al., 2010) and low intensity repetitive transcranial magnetic stimulus (Makowiecki et al., 2014) show that the secretion in brain derived neurotrophic factor (BDNF) increases after application of stimulation. BDNF secretion has been associated with increase in overall responsivity (Lu, 2003) and can also explain tDCS-induced BOLD signal changes (Kar and Wright, 2014). Hence tACS-induced elevation in BDNF might be improving sensitivity in a frequency independent manner. Second, a reduction in spike rate adaptation under the influence of membrane voltage fluctuations has been previously reported in vitro (Fernandez et al., 2011). Fernadez and colleagues attributed this effect to slow de-inactivation of Na^+ channels. In addition, slow hyperpolarization activated Na^+ and Ca^{2+} dependent K^+ channels have been implicated in the induction of adaptation (Sanchez-Vives et al., 2000a). It is possible that tACS disrupts the recruitment of these slow channels and thereby reduces adaptation. It should be noted that the two proposed mechanisms are not mutually independent. For instance, a tACS-induced increase in BDNF level could increase neuronal excitability by depolarizing the membrane voltage which will therefore hinder the recruitment of the slow hyperpolarization activated potassium channels.

Comparison of tDCS and tACS mechanisms

Standard tDCS protocols (Nitsche et al., 2008) involve prolonged periods (~20 minutes) of tDCS application. Previous studies suggest that the electrophysiological effects of tDCS needs some time to develop (Fritsch et al., 2010). Fritsch et al. (2010) demonstrated in-vitro in mouse M1 slices that the onset of the effects (BDNF dependent potentiation of functional excitatory post synaptic potentials) had a latency of several minutes and the offset outlasted the application time. This predicts that the intermittent short-term (~4s) application of tDCS (as applies to our paradigm) should be insufficient to induce any significant electrophysiological and thereby behavioral effect. In vitro studies in rat M1 slices also suggest that uniform electric field stimulation can produce somatic polarization (Radman et al., 2009). This polarization is much stronger for pyramidal cells than inhibitory cells due to morphological differences that render the latter less susceptible to uniform fields. On the other hand in vivo recordings from rats show that application of tACS entrains cortical unit activity irrespective of cell type (Ozen et al., 2010). In addition, our results also show that tACS-induced behavioral effects can be produced with much shorter application time. Taken together, these differences put tACS at a practically advantageous position over tDCS.

CHAPTER 5

Transcranial alternating current stimulation attenuates neural adaptation in area MT of the macaque

In chapter 3 and 4, I have presented a robust behavioral effect of 10 Hz tACS; attenuation of motion adaptation. In this chapter, I present neural data recorded from awake, behaving macaques. I have explicitly tested the hypothesis that tACS reduces visual motion adaptation-induced effects in motion sensitive neurons in area MT of the macaque. This work has been submitted for publication.

Pending publication of journal articles included in the chapter:

Kar, Kohitij, Jacob Duijnhouwer, and Bart Krekelberg. "Attenuating adaptation: a novel mechanism for tACS." *Nature Neuroscience* (submitted).

5.1. Abstract

The noninvasive neuromodulation technique transcranial alternating current stimulation (tACS) has recently generated renewed interest. A multitude of recent reports have demonstrated the behavioral efficacy of tACS, ranging from suppression of Parkinsonian tremors (Joundi et al., 2012), enhanced memory consolidation (Marshall et al., 2006) to changes in risk seeking behavior (Sela et al., 2012). Moreover, in-vivo (Ozen et al., 2010; Ali et al., 2013) and in-vitro (Reato et al., 2010) studies show that externally applied alternating electric fields can entrain ongoing brain oscillations, thereby manifesting tACS as a promising tool for neuromodulation. Despite its widespread use in cognitive neuroscience and the clinic, a complete understanding of the electrophysiological effects of tACS on the intact brain is still lacking (Herrmann et al., 2013). We previously reported that the application of tACS during adaptation to visual motion attenuates the motion aftereffects in humans (Kar and Krekelberg, 2014) . Here we measured directly the effects of tACS on the neural coding of visual motion in the middle temporal (MT) and medial superior temporal (MST) cortex of awake, behaving macaques following adaptation to motion. tACS mitigated the effects that motion adaptation has on the neuronal tuning amplitude, width and evoked local field potentials. Our results confirm that tACS interacts with the stimulus evoked adaptive processes in the neurons. This property of tACS can be utilized to target it at specifically adapted brain areas or to selectively reduce adaptation in brain areas. Our approach also establishes the awake, behaving macaque as an animal model to study tACS. Specifically, this important step now allows us to relate tACS-induced behavioral

changes directly to neural changes, thereby providing a mechanistic insight into the neural mechanisms of action of tACS.

5.2. Introduction

Transcranial alternating current stimulation (tACS) produces acute perceptual (Struber et al., 2014), motor (Joundi et al., 2012) and cognitive (Marshall et al., 2006; Sela et al., 2012) changes in humans. Due to the paucity of studies probing the underpinnings of these effects in the intact brain (Herrmann et al., 2013; Reato et al., 2013), it remains unclear how these behavioral effects are generated. As a consequence, development and application of this promising technique for noninvasive neuromodulation is mainly based on trial and error. To address this issue we use a non-human primate model to directly measure the neural consequences of tACS.

We have recently shown that tACS (10 Hz; 0.5mA) applied over area hMT+ in human subjects result in an increase in sensitivity for coarse motion discrimination and a reduction in the strength of the motion aftereffect (Kar and Krekelberg, 2014). We argued that tACS could cause both these behavioral effects if it attenuated adaptation in motion sensitive neurons. Here we investigate this neural hypothesis. There is strong evidence that motion discrimination as well as the behavioral consequences of motion adaptation are linked to neural activity in the middle temporal (MT) area of the macaque brain (for review see Parker and Newsome, 1998). Given the well-established homologies between the macaque

and human visual system (Orban et al., 2003), our behavioral findings therefore naturally lead us to investigate the influence of tACS in area MT of the macaque.

We recorded extracellular signals in area MT while applying transcranial alternating current stimulation using scalp electrodes. We investigated changes in individual neurons' firing rates as well as measures of synchronous population activity reflected in local field potentials (LFPs). To avoid misinterpreting electrical artifacts from stimulation as changes in neural response we restricted our analysis to the period following transcranial stimulation. Our data provide strong support for the novel view that tACS attenuates adaptation. The effect of tACS on the tuning parameters of neurons was proportional to the amount of adaptation induced in the neurons. We also observed an adaptation specific change in the stimulus evoked LFP (80 -120ms latency) components with tACS. Furthermore, we observed a broadband increase in LFP power (10-120Hz); an adaptation independent effect of tACS.

5.3. Results

We recorded extracellularly from 107 motion-selective MT/MST neurons in two *Macaca mulatta.* The tACS electrodes were placed on the scalp over the superior temporal sulcus, one electrode on either side of the implanted recording chamber (Figure 5.1a). The monkeys were trained to fixate a dot at the center of the screen and maintain fixation while moving random dot stimuli were presented in the neuron's receptive field.

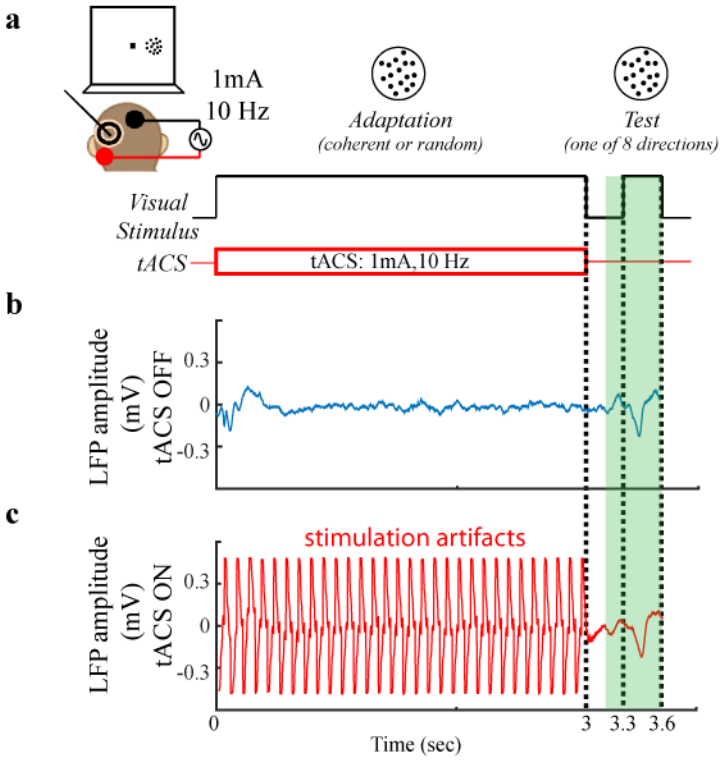

Figure 5.1 Experimental setup and procedure. a) Visual paradigm. On each trial a RDK (random or coherent motion) was presented for 3s followed by a blank period of 300 ms, followed by a 300 ms coherent RDK (at one of eight evenly spaced directions). Monkeys fixated a dot at the center of the monitor screen. RDKs were presented at the center of the RF of the cell being recorded. Two tACS electrodes were placed on either side of the recording chamber. b) Local field potentials recorded during an example trial in the random motion condition without tACS. c) Local field potentials recorded during an example trial in the random motion condition with tACS are dominated by stimulation artifacts. To avoid contamination from these artifacts, we only analyzed data obtained at least 150 ms after tACS offset (green period).

Based on our previous behavioral findings (Kar and Krekelberg, 2014), we hypothesized that tACS would interfere with the induction of adaptation. We therefore measured direction tuning curves in a strongly adapted state (i.e. after

adaptation to 3 s of coherent motion) and in a weakly adapted state (after adaptation to 3 s of random motion; we refer to this condition as unadapted, see Materials and Methods). To investigate the influence of tACS on the induction of adaptation, tACS (1 mA, 10 Hz) was applied during the adaptation period in half of the trials. The strong stimulation artifacts (Figure 5.1c) prevented a meaningful analysis of the extracellular recordings during the adaptation period, and we analyzed only the data obtained at least 150 ms after tACS offset (Figure 5.1b and c).

tACS changed tuning curves of single neurons

Figure 5.2 shows the tuning curves of two well-isolated example neurons. In the neuron shown in Figure 5.2a, adaptation to coherent motion (adapt, blue curve) led to smaller response amplitudes than adaptation to random motion (unadapt, black curve). When adaptation was combined with tACS, this amplitude suppression was approximately halved (adapt^{tACS}, red curve). Figure 5.2b shows an example neuron in which tuning amplitude increased after adaptation (Figure 5.2b). In this neuron, concurrent tACS with adaptation led to a smaller increase in firing rate (Figure 5.2b, red curve). Both examples show that tACS attenuated the effects of adaptation.

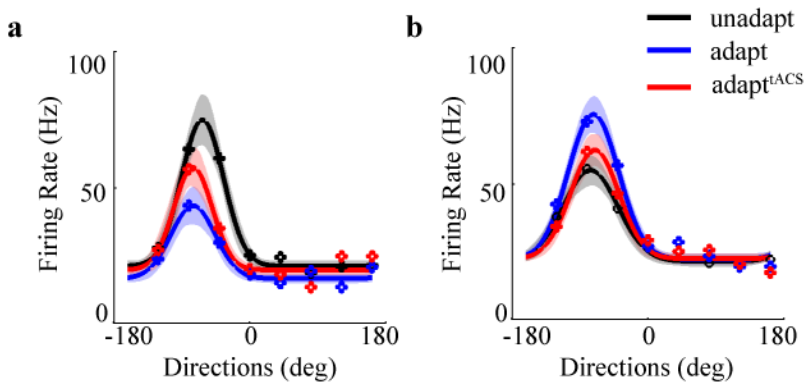

Figure 5.2 tACS-induced effects on neuronal tuning curves. a) Tuning curve estimates of an example neuron in three conditions (black–unadapt; blue–adapted; red–adapted with tACS). tACS attenuated the adaptation-induced reduction in tuning amplitude. b) Tuning curve estimates of a second example neuron. tACS attenuated the adaptation-induced facilitation in tuning amplitude. Shaded regions show standard error.

tACS effects depended on the level of adaptation

To demonstrate that this was consistent across the population, we estimated the tuning amplitude and width for each of the four tuning curves per neuron. Figure 5.3 shows the relation between the adaptation-induced change in amplitude (horizontal axis in Figure 5.3a) and the effect of tACS (vertical axis). The correlation between these measures was significantly below zero (Spearman correlation $\rho(107) = -0.61$; $p < 0.001$). This negative correlation shows that irrespective of the direction in which adaptation changed the peak of the tuning curve, tACS changed the peak in the opposite direction. Hence this supports our hypothesis that tACS attenuated adaptation. Figure 5.3b shows the analogous population analysis for changes in the width of the tuning curve. In neurons whose

tuning curve was strongly broadened by adaptation, tACS led to a narrowing of the tuning curve (and vice versa). This correlation was also significantly below zero ($\rho(107) = -0.7$; $p < 0.001$), and provides additional support for the hypothesis that tACS attenuates adaptation.

An alternative hypothesis for the tACS-induced changes in tuning curves could be that tACS generates an unspecific change, unrelated to adaptation (e.g. an arousal or attentional signal that varied across neurons). If this were the case, one would expect tuning curve changes to be similar when tACS was applied in the adapted and unadapted conditions. Our data do not support this hypothesis. Figure 5.3c and d show that, across the population, the tACS-induced tuning changes in the unadapted conditions were not correlated with the changes in the adapted conditions.

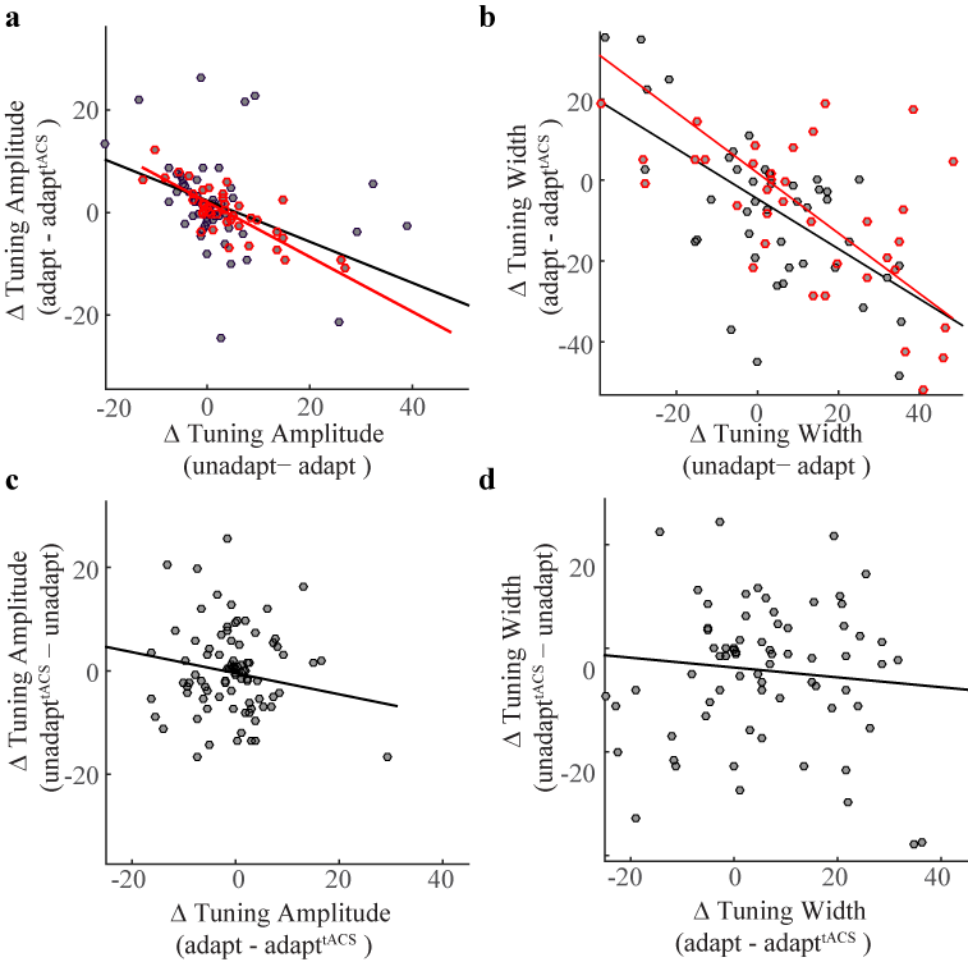

Figure 5.3 Population analysis of tACS-induced changes in tuning properties. A) Comparison of the tuning amplitude change induced by tACS with the tuning amplitude change induced by adaptation. Each dot represents a single neuron. Red lines show the result of a robust linear regression. Red dots show the neurons that were adapted near their preferred direction. B) Same as A, but comparing changes in tuning width. C) Comparison of the tACS-induced change in tuning amplitude in the unadapted conditions with tACS induced change in tuning amplitude in the adapted conditions. D) Same as C, but comparing changes in tuning width. This figure shows that the tuning curve changes induced by adaptation (and only those changes) are partially undone when adaptation is combined with tACS. In other words, tACS consistently attenuated adaptation.

If tACS indeed interferes with the induction of adaptation, then one would expect the largest effects of tACS to occur when adaptation is strong. Figure 5.3 supports this view on a cell-by-cell basis, but our recordings also allow us to investigate this in a somewhat different manner. Adaptation effects are known to be strongest when the adapting stimulus is similar to the preferred stimulus (Kohn and Movshon, 2003; Krekelberg et al., 2006b) . Because we recorded multiple neurons at the same time (and because our online estimate of the preferred direction was relatively coarse; see Methods), some neurons were adapted with their preferred direction of motion, while others were adapted with a direction of motion on the flank of their tuning curve.

For Figure 5.4 we grouped the neurons by the difference in their preferred direction and the direction of the coherent adapter. As expected (Kohn and Movshon, 2003), neurons showed the strongest reduction in tuning amplitude when they were adapted with coherent motion within 45° of their preferred direction (black curve, Figure 5.4a). In agreement with the attenuation hypothesis, the effect of tACS (see Methods) was largest for these neurons (red curve, Figure 5.4a). Neurons exposed to an adapter on the flank of their tuning curve adapted less, and tACS had less of an effect. The analogous relationship for changes in tuning width is shown in Figure 5.4b. This analysis confirms our hypothesis that tACS effects depend on the level of adaptation.

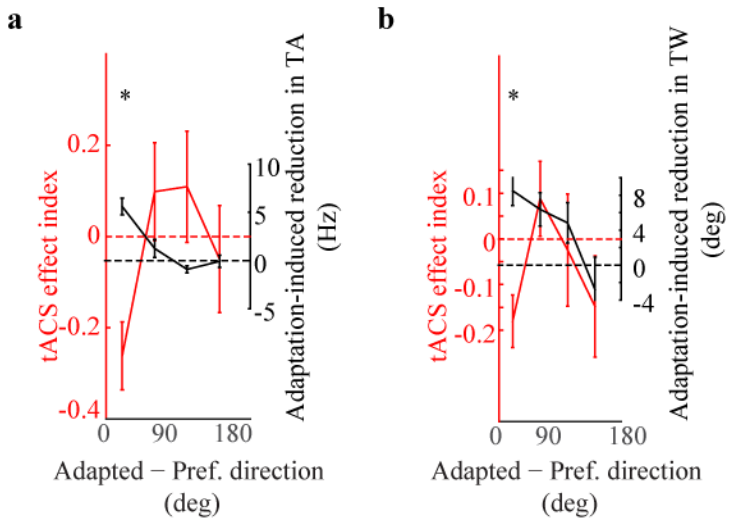

Figure 5.4 tACS-induced effects depended on the level of adaptation. a) The black curve shows the reduction in tuning amplitude (TA) after adaptation as a function of the difference between the adapter direction and the preferred direction of the neuron. The red curve shows the effect of tACS on TA following adaptation. '*' indicates a significant difference ($p<0.05$) from 0. b) same as a) but now for adaptation/tACS-induced changes in tuning width (TW). This figure shows that the effect of tACS was large when the effect of adaptation was large; tACS attenuated adaptation.

tACS modulated evoked responses

We used the local field potentials to gain insight into tACS-induced changes in aggregate population activity. Figure 5.5a shows the evoked LFPs following the test stimulus, averaged over all trials and recording sites (see Materials and Methods). The magnitude of the evoked LFP during the test interval was larger when adaptation was combined with tACS (red curve) than in the adaptation without tACS condition (blue curve). This effect was strongest in the first negative deflection (N1). Based on previous findings (Hoffmann et al., 1999) that adaptation leads to a specific reduction of the second negative deflection of the evoked

potential (N2), we also analyzed the subset of sites at which the N2 after adaptation was reduced (compared to the unadapted condition). In those sites, pairing tACS with adaptation led to a strong and statistically significant increase in N2 (Figure 5.5b). In other words, in sites at which adaptation (as measured by the reduction in N2) was strong, tACS significantly attenuated adaptation (there was less of a reduction in N2). A comparison of the unadapted conditions with and without tACS showed an increase in both N2 and N3 that was qualitatively similar in the sites that adapted strongly (Figure 5.5c and d). This demonstrates that some tACS induced changes in the evoked potential do not require strong adaptation.

tACS increased broadband spectral power

One of the potential advantages of tACS over direct current (tDCS) or transcranial magnetic stimulation is that it may be able to entrain specific cortical rhythms. We investigated this claim using spectral analysis of the LFP. To avoid contamination from stimulation artifacts, we only considered LFPs recorded at least 150 ms after the offset of stimulation.

To quantify the spectral content during test stimulus presentation, we removed the average evoked response from each trial and then estimated the spectral power per frequency band (see Materials and Methods). Figure 5.5e shows that spectral power over a broad range of frequencies was larger after tACS in both the adapted and unadapted conditions. This same broadband increase in power was also observed in the spectral content of the spontaneous LFP recorded in the 150 ms before presentation of the test stimulus (not shown). Statistically, we analyzed these data per frequency band using a two-way analysis of variance with factors

of adaptation (coherent/random) and stimulation (tACS/no-tACS). The main effect of tACS was significant both during and before test stimulus presentation, and in each frequency band ($F(1,1) > 5$; $p < 0.05$). The main effect of adaptation or the interaction did not reach significance in any frequency band or window ($F < 0.02$; $p > 0.05$). This demonstrates that tACS induced a broad band increase in spectral power in the spontaneous activity that outlasted tACS offset by at least 300 ms.

tACS did not evoke long-lasting frequency-specific entrainment

Given that our tACS frequency was 10 Hz one might predict entrainment specifically in the alpha band. Figure 5.5e shows little evidence of such frequency-specific entrainment, but we tested this hypothesis quantitatively by first calculating the ratio of the power in the tACS conditions with the corresponding no-tACS conditions per frequency band. This approximately equalized the variance across conditions and enabled us to perform an ANOVA with frequency as a factor. The main effect of frequency was not significant either before or during test stimulus presentation ($F(4)=0.01$; $p > 0.05$). This shows that the increase in spectral power was indeed broadband and that there was no evidence of long-lasting, frequency-specific entrainment of neural activity after tACS offset.

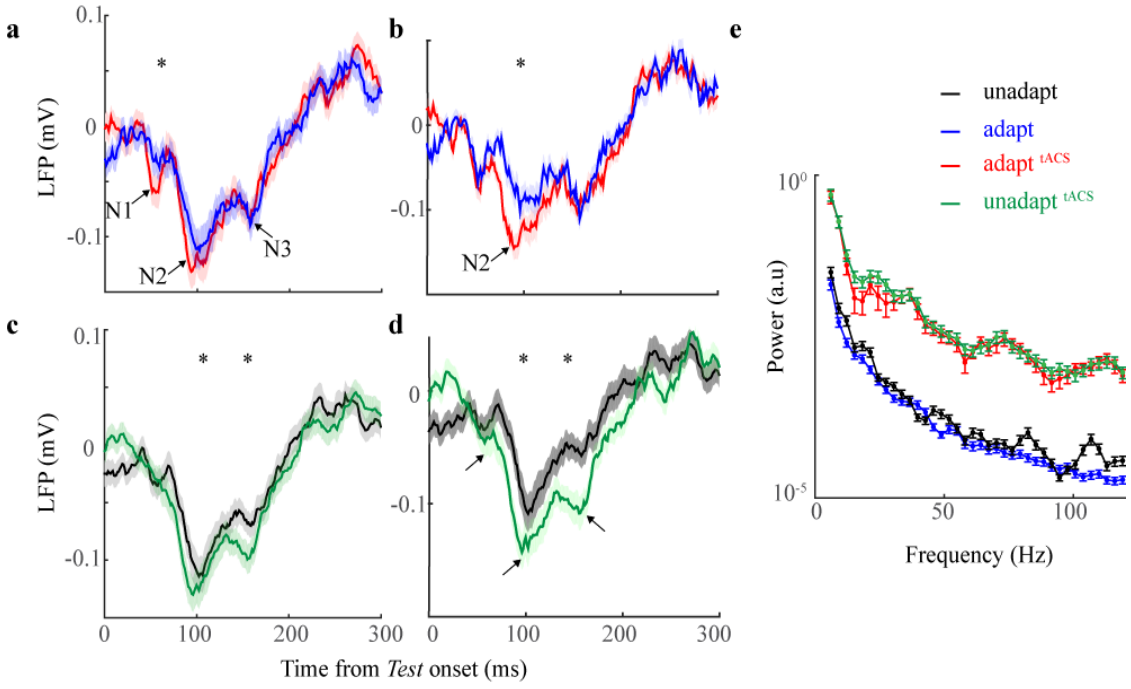

Figure 5.5. The influence of tACS on local field potentials. a) The evoked LFP in the test period after adaptation (blue) and after adaptation paired with tACS (red). N1, N2, and N3 refer to the first, second, and third negative deflection of the LFP. Data are averaged over all sites (N=76). Shading shows standard errors. Asterisks indicate a significant difference between the two conditions at that point in time (see Methods). b) Same as a), now only for sites in which the N2 component was reduced by adaptation (see Methods). c) Evoked LFP response in the unadapted condition (black), and in the unadapted + tACS condition (green). d) Same as c, averaging only over sites in which the N2 component was reduced by adaptation. e) Power spectrum of the LFP signal in the test period, after subtracting the evoked response. This figure shows an increase in evoked responses after tACS, and a broadband increase in LFP power, but no evidence for a long-lasting, frequency-specific entrainment of the LFP signal.

5.4. Discussion

Our results show that tACS attenuated the effects of visual motion adaptation in motion-selective neurons. This was supported by tACS-induced changes in the peak and width of the tuning curves of single neurons, as well as the strength of the evoked responses; all of these changes were particularly pronounced when adaptation was strong. In addition, we show that some tACS-induced neural changes appear to be independent of adaptation. Of these, a broadband increase in spectral power in the LFP that persisted for at least 300 ms after tACS-offset was most noticeable.

We first discuss our findings in light of prior reports on adaptation and tACS, address potential confounds and the potential of the non-human primate as an animal model to study tACS, and conclude with a brief discussion about possible cellular mechanisms of tACS supported by our findings.

Adaptation

Even though adaptation is traditionally associated with a reduction in peak firing rate, more recent work has shown that adaptation can also increase firing rate in V1 and MT (Patterson et al., 2014). Our data provide further experimental support for this view. On average, our sample of neurons had a lower peak firing rate after adaptation, but many neurons individually increased their firing rates (See Figure 5.2b). The mechanisms underlying this complexity are not fully understood, but it seems likely that adaptation of the surround and subsequent disinhibition (Wissig and Kohn, 2012) and the complex consequences of reducing the firing rate of a subset of neurons in a recurrently connected network (Richert et al., 2013) are

involved. This complexity has potential consequences for the fMRI adaptation method which typically assumes that firing rate can only go down after adaptation (Krekelberg et al., 2006a), as well as for our general understanding how the brain reacts to changes to its recent sensory experience (Clifford et al., 2007).

tACS in non human primates

The non-human primate provides a unique opportunity to study how transcranial stimulation affects neural processing. Given the gross physical and anatomical similarities, current spread in the macaque is expected to be more similar to the human brain than, for instance, in the lissencephalic rodent brain. Moreover, macaques can be trained to perform complex behavioral tasks and these can be used in combination with tACS to strengthen the link with findings in humans.

The surgical implants needed to perform intracranial recordings inevitably modify the induced fields and this could in principle change the effect of tACS. However, both computational models (Miranda et al., 2006; Laakso and Hirata, 2013) and behavioral studies (Kar and Krekelberg, 2012), predict broad intracranial current spread, hence one can be relatively certain that at least some induced fields reach most of the cortex regardless of the physical details of the implants. Our finding that tACS changes neural responses in area MT support this view. Moreover, given that our electrophysiological results were at least broadly consistent with our earlier behavioral findings, the differences between the electric fields we induced in the macaque and human must have been relatively insignificant in terms of the overall neural effects they evoked. Nevertheless, we believe it is important to

explore the details of the induced intracranial fields, and we are actively exploring the validation and further development of techniques that can target brain areas more specifically (Dmochowski et al., 2011).

Phosphenes

In nearly every electrode montage, tACS at 10 Hz and 1 mA evokes phosphenes in most humans and these phosphenes have a retinal origin (Kar and Krekelberg, 2012). This is a potentially problematic confound for many tACS studies as the phosphenes generate an additional visual input, or they can change the subject's attentional or arousal state. We have previously argued (based primarily on the peripheral location of the phosphenes and the hemispheric lateralization of the behavioral effects (Kar and Krekelberg, 2014) that the attenuation of adaptation is unlikely to be caused by phosphenes. Our current electrophysiological findings add additional arguments against the hypothesis that a generalized change in attention/arousal/alertness is solely responsible for the behavioral and neural consequences of tACS. Specifically, we found that tACS-induced changes in the unadapted condition were not correlated with tACS-induced changes after adaptation to coherent motion (**Figure 5.3c and d**). Such stimulus specificity seems difficult to explain in a framework in which tACS only changes the level of arousal.

Entrainment

Evidence supporting the claim that tACS entrains neural activity has now been obtained in anesthetized ferrets (Ali et al., 2013), awake rats (Ozen et al., 2010),

and humans (Helfrich et al., 2014). The animal experiments (including ours), however, report that there is no significant, long-lasting entrainment after tACS offset (Ozen et al., 2010; Ali et al., 2013) . Contrary to this, Helfrich et al. (2014) recently reported that application of tACS at 10 Hz entrained the scalp EEG ~1 minute after tACS offset. There are a number of possible explanations for this discrepancy. First, it is possible that the longer period of continuous stimulation (20 min) in the Helfrich et al.(2014) study led to such strong entrainment. Second, the human subjects had a strong ongoing alpha rhythm even before stimulation whereas such a peak in the response was not present in our recordings (not shown). It may be easier for tACS to boost an already present dominant rhythm than establish one de-novo (Ali et al., 2013). The third possibility is a potentially confounding factor of time in the human EEG experiments: post-tACS EEG measurement always followed post-sham EEG measurement by ~40 minutes. This implies that the increase in alpha power may have been due to increased drowsiness. The increase in alpha during sham stimulation (Figure 5.3c in Helfrich et al., 2014) provides some experimental support for this interpretation. In our study tACS and no-tACS blocks were randomly interleaved, hence no such confound exists.

Attenuation of adaptation by tACS

At the current levels generally considered safe (<2 mA), tACS generates intracranial electric fields on the order of 1 V/m, and membrane potential changes on the order of at best a few mV. This small effect has led to some skepticism about the efficacy of tACS. However, it has been shown that even small (<2mV)

membrane voltage fluctuations reduce spike frequency adaptation in rat hippocampal CA1 neurons (Fernandez et al., 2011). We speculate that in our recordings the small tACS-induced membrane fluctuations may have similarly prevented the activation of sodium or calcium activated potassium channels (Sanchez-Vives et al., 2000a; Wang et al., 2003) in visual cortical neurons. This would attenuate those neurons' adaptation (Sanchez-Vives et al., 2000a) and thereby indirectly cause much larger changes in firing rate than expected from a few millivolts of membrane polarization. This hypothesis could be tested in-vitro.

The attenuation of adaptation hypothesis also provides some insight into the question how tACS can generate electric field changes throughout the brain (Laakso and Hirata, 2013) but nevertheless have specific, non-diffuse effects. Notably, if tACS affects only adaptation, then it will affect only those neurons that are undergoing adaptation at the time of tACS stimulation. This implies that the subset of affected neurons can be changed by changing the experimental task that the subject performs while undergoing tACS. In other words, to target an area, the experimenter can choose to adapt it with a relevant stimulus or task, which will make it more susceptible to tACS.

5.5. Materials and Methods

Two adult male Rhesus monkeys (Macaca mulatta) participated in these experiments. Experimental and surgical protocols were approved by the Rutgers

University Animal Care and Use Committee and complied with guidelines for the humane care and use of laboratory animals of the National Institutes of Health.

Surgical procedures and electrode location

All surgical procedures were conducted under sterile conditions using isoflurane anesthesia. Titanium head posts (Gray Matter Research) were attached to the skull using titanium bone screws. Custom made high-density polyethylene recording chambers were implanted normally to the skull, and dorsal to the expected location of MT. We confirmed recording locations in area MT on the basis of structural magnetic resonance images obtained after implantation, as well as on the basis of physiological criteria such as the high prevalence of direction selective responses, and the relatively small receptive fields (compared to neighboring area MST).

Recording

Visual stimulus generation, the triggering of tACS, and data acquisition were under the control of our in house software for visual experimentation: Neurostim (http://neurostim.sourceforge.net). Stimuli were presented on a CRT monitor (Sony FD Trinitron) spanning 30 x 40 degrees at a resolution of 1024 x 768 pixels and a refresh rate of 150 Hz.

At the beginning of each recording session, we punctured the dura mater with a sharp, metal guide tube to allow access to the cortex. The guide tube or one of the head screws served as the ground for the electrode signal. We used a micro-

positioner (NAN Instruments, Nazareth, Israel) to lower a parylene coated tungsten electrode (1.5 MΩ; FHC Inc., Bowdoin, ME) into area MT through the guide tube. We manually isolated single cells by listening to their visually driven response which was made audible on a speaker while the monkey observed moving stimuli (see section "Experimental procedure"). The raw signal was sampled at 25 kHz using Alpha Lab (Alpha-Omega Engineering, Nazareth, Israel). To extract spikes we first band-pass filtered the raw signal between 300 Hz and 6 KHz, and then applied a threshold equal to 4 standard deviations of the filtered signal . We used KlustaKwik (Harris et al., 2000) to cluster these waveforms into separate units (up to three, significantly direction tuned units were used per recording depth). Local field potentials (LFP) were extracted from the raw signal by first band-pass filtering between 1 and 120 Hz and then resampling at 782 Hz.

Eye movements were recorded using an infrared eye tracker (Eyelink2000; SR Research). Trials in which eye position deviated from the fixation point by more than 1 degree were not used in the analysis.

Transcranial stimulation

tACS was delivered with an STG4002 stimulus generator (Multi Channel Systems, Reutlingen, Germany) through 3.2 cm x 3.2 cm reusable surface electrodes (uni-tab electrodes). The applied current was always sinusoidal with a 1.0 mA amplitude and 10 Hz frequency.

One tACS electrode was placed immediately between the ear and the recording chamber, adjacent to area MT (in the left hemisphere for monkey N and in the right hemisphere for monkey M). The other electrode was placed 4 cm anterior to the

vertex (standardized non-human primate Cz location, homologous to human Cz location based on 10-20 EEG system). To improve skin conductivity at the site of the electrodes, we applied a mixture of water, isopropanol and aluminum chlorohydrate to the area of the scalp. We could not replicate the human electrode montage used by Kar and Krekelberg (2014) with the macaques due to the location of the recording chamber and the head post screws (see Discussion).

Experimental Procedures

In each experiment, the monkey started a trial by bringing its gaze within an invisible 2 x 2 ^{o} window surrounding a small red dot that was permanently present at the center of the screen. The monkeys were rewarded with apple juice for maintaining fixation throughout each trial.

In each recording session, we ran two mapping experiments to guide stimulus location and motion direction of the main tACS experiment. First, we determined the preferred direction of the neuron using a sparse full screen pattern of dots that moved along a circular path resulting in a uniform translational velocity (Schoppmann and Hoffmann, 1976; Krekelberg, 2008b; Hartmann et al., 2011). Second, we determined the spatial receptive field using localized motion pulses in the preferred-direction in a matrix of 4x3 patches covering the screen. In the main experiment, the stimuli were centered on the patch that elicited the maximum mean response.

In the main experiment, trials consisted of a 3 s adapter stimulus followed by a 300 ms blank period in which only the fixation dot was visible, and a 300 ms test

stimulus. Both the adapter and test stimulus consisted of 700 anti-aliased dots (30 cd/m^2, effective diameter 1.5 pixels) on a 4 cd/m^2 background, moving within a 5^o radius circular aperture.

The main experiment used a 2x2 factorial design to test the hypothesis that tACS attenuates adaptation induced changes. The first factor was the level of motion adaptation, which we manipulated by choosing the adapter stimulus. Each of the dots in the adapter stimulus either moved in a randomly chosen direction, or they all moved in the neuron's preferred direction. The random motion stimulus is known to induce much less adaptation than the coherent motion stimulus, hence for ease of reference we will use the term unadapted for the former, and adapted for the latter condition. The second factor was the presence or absence of tACS (10 Hz, 1.0 mA); in tACS-ON trials, it was only applied during the 3s that the adapter stimulus was on the screen. In the tACS-OFF trials it was not applied at all.

The dots in the test stimulus moved coherently in one of eight evenly spaced directions spanning the circle. This allowed us to measure a direction tuning curve under each of the experimental conditions. The four conditions of the factorial design were presented in separate blocks with one repeat per test-direction. The blocks were randomly interleaved and repeated at least 10 times.

Data Analysis

Tuning Curves

Our primary interest was to determine how tACS affected direction tuned responses. We used the average response (firing rate) of a neuron during the 300 ms test interval to estimate tuning curves, separately for each of the four conditions of interest (coherent-adaption/random-adaptation x tACS-ON/tACS-OFF). Using a resampling based Bayesian method(Cronin et al., 2010) we estimated tuning amplitude (TA), tuning width (TW), baseline firing rate (BS**)** and preferred direction (PD) of a circular Gaussian tuning curve. From these measures we also extracted the responsivity: the difference between tuning amplitude and its baseline firing rate (TA-BS).

Correlation Analysis

Our behavioral results (Kar and Krekelberg, 2014) show that the influence of tACS depends on the strength of adaptation. To investigate the neural basis for this effect we determined the Spearman correlation (ρ) between the change in tuning amplitude due to tACS ($TA_{tACS+coh\_adap} - TA_{coh\_adap}$) and the change in amplitude due to adaptation ($TA_{coh,adap} - TA_{noise\_adap}$) (refer Figure 5.3).

Note that these two measures both depend on coherent motion adaptation without tACS (TA_{coh_adap}), and are thus not mutually independent. This precludes the use of standard significance testing of Spearman's ρ. Instead, we used a permutation test. Our observed data (tuning amplitudes) can be treated as a matrix with N rows and M columns, where N is the number of recorded cells and M is the number of

experimental conditions (column 1: unadapted, column 2: adapted and column 3: adapted with tACS). Hence to estimate ρ =corr(column 1 - column 2, column 2 - column 3), we computed the null distribution of correlations by randomly shuffling the data matrix 1000 times and estimating ρ for each shuffle. To test for significance, we compared the actual ρ with 95th percentile of the null distribution. The same analysis method was used for the tuning width data.

For the data presented in Figure 5.4, the neurons were first grouped according to the difference of their preferred direction to direction of the coherent adapter. Then the above analysis was performed on each group. Each value plotted in the blue curve is the difference between the mean of the null distribution and the actual ρ for each group.

LFP Analysis

Local field potentials (LFP) were extracted from the raw signal, sampled at 782 Hz and then band-pass filtered between 1 and 120 Hz. The evoked responses were determined by averaging the LFP from test stimulus onset over all trials in which the test direction was closest to the adapting direction. For the average evoked LFP shown in Figure 5a-d, we averaged the evoked LFPs across all 76 recording sessions. We defined the negative peaks N1, N2 and N3 as the minimum LFP values between 40-60 ms, 80-120 ms and 150-200ms respectively. We used the non-parametric, Wilcoxon signed rank test to test if the negative peaks were significantly different ('*' in Figure 5.5 a-d) under two separate conditions.

For the spectral analysis, we focused on the LFP trace recorded 150 ms post tACS offset. For each recording site, we first calculated the mean evoked LFP for each of the four conditions (coherent-adaption/random-adaptation x tACS-ON/tACS-OFF). We then projected (inner product) each LFP time series (for each trial) data onto the mean evoked LFP response for the respective condition and subtracted out the component. Thus, we removed the evoked component from each raw trace. Multi-taper spectrograms were estimated using used the Chronux software package (http://www.chronux.org) with parameters: time bandwidth product = 1.2, number of tapers = 2, sampling frequency = 781.25 Hz. We divided the frequencies into five non overlapping bands, alpha (8-15 Hz), beta (15-30 Hz), low gamma (30-50 Hz), medium gamma (50-80 Hz) and high gamma (80-120 Hz). We analyzed each frequency band using a separate two-way analysis of variance with factors of adaptation (coherent/random) and stimulation (tACS/no-tACS).

CHAPTER 6

General Conclusion and future directions

The work presented in this thesis was undertaken to investigate the mechanisms of transcranial electrical stimulation. The results of my thesis highlight two main properties of tES-induced effects. First, the electric field induced by tES spreads well beyond the area of application. Second, tACS attenuates the behavioral and neural effects of motion adaptation.

In the subsequent sections, I will discuss the main findings of the thesis, consider their significance with respect to the current state of research in tES and end with a discussion of the future directions.

6.1. Current spread and entrainment of neural population during tES

In chapter 2, I have shown that phosphenes perceived during application of tES over the visual cortex, are produced by electrical stimulation of the retina, due to volume conduction of the applied field through the scalp. The results of this study suggest that the current density (~0.05 mA/cm^2) at typical tES current levels (~1 mA) do not create large enough fields to produce suprathreshold stimulation of the underlying cortex. Most of the current spreads well beyond the area of

application. This result has been further confirmed by modelling studies (Laakso et al., 2014). However, it is possible that tES produces sub threshold modulations (in the order of 0.2 mV) and, in case of tACS, these could synchronize ongoing oscillations, as predicted by multiple prior reports (Ali et al., 2013). In addition, weak electric field modulations can be strengthened by network activity (Francis et al., 2003) and produce a significant behavioral change. However, the study presented in chapter 5 failed to report any frequency specific entrainment with 3 seconds of tACS application. There is a significant broadband increase in the power of the frequency components of the local field potentials after tACS. The underlying mechanism behind this increase is unknown. This global increase in power is not reflected in the spike rate of the neurons (as observed in chapter 5). Hence, whether this increment in LFP power has any direct behavioral consequence remains an open empirical question.

6.2. Attenuation of cortical adaptation with tES

In chapter 3, I reported that tES (10 Hz) reduced the motion after-effect and also improved motion discrimination sensitivity. In chapter 5, I recorded directly from visual motion direction selective neurons in area MT of the macaque. tES attenuated the effects of visual motion adaptation in the MT and MST neurons . Taken together, these findings can be summarized succinctly as demonstrating that tES attenuates adaptation. Furthermore, adaptation has been associated with redundancy reduction (Barlow and Foldiak, 1989) and efficient coding (Adibi et al., 2013) of information. From this perspective, reduction of adaptation, therefore

makes application of tES an undesirable manipulation. However, as shown in chapter 3 and 4, alleviation of adaptation helps improve coarse direction discrimination. Therefore it is possible to harness the changes induced by tES in a positive way in order to benefit human performance in cognitive tasks. Apart from that, adaptation can also be used as a tool to make a specific brain area more prone to tES. For instance, application of tES to aid stroke recovery in the motor cortex has been reported (Schlaug et al., 2008). Specific parts of the motor cortex control the movement of different areas of the body. Hence it is possible that adapting a certain area of the motor cortex with a relevant task might make that area more prone to tES. In addition, brief periods of adaptation have been shown to have long term cognitive effects (Vul et al., 2008). Hence I speculate that long term effects of the tACS–induced reduction in adaptation may account for the long lasting effects of tACS itself.

6.3. Mechanisms of tACS

The electric field induced by tACS is not limited to the area directly underneath the electrode. Therefore it is difficult to predict whether the behavioral effects of tACS originate at any specific brain region. However, given that tACS specifically attenuated motion adaptation, both behaviorally and in single neurons, I propose a cellular mechanism of tACS. Contrast adaptation in the cat visual cortex has been previously attributed to the recruitment of an intrinsic membrane hyperpolarization (Sanchez-Vives et al., 2000b). This adaptation-induced hyperpolarization of the membrane potential was mainly attributed to sodium and calcium dependent potassium currents (Sanchez-Vives et al., 2000a). I speculate

that the membrane voltage fluctuations produced by tACS directly interacts with the dynamics of the Na^+ and Ca^{2+} activated K^+ channels, thereby reducing the after effect of adaptation. This hypothesis can be explicitly tested in vitro. Specific genes termed slick and slack genes have been identified that encode for these sodium activated potassium channels (K_{Na}). Recently mouse visual cortical cells have been shown to exhibit adaptive properties like that of the macaques and cats (Stroud et al., 2012). Future studies can utilize slick and slack knockout mice to test how the lack of these genes modify the efficacy of tACS. It is important to note that the proposed cellular mechanism doesn't exclude possible network effects of tACS. Effects of weak electric fields can intensify due to network interactions (Francis et al., 2003). Therefore, tACS might entrain neural networks, which leads to the reduction of adaptive changes at a single neuron level. These hypotheses need to be explicitly tested in future studies.

6.4. Do we need focal stimulation?

Most of the recent advances in the field of tES push for developing electrode montages and techniques to ensure more focal stimulation (Dmochowski et al., 2011). The possibility of selectively modulating a specific brain area noninvasively is extremely desirable. However it undermines the success of the regular large sized conventional pad electrode in being so effective. Hence the question still exists whether the global stimulation delivered by these pads is crucial for the clinical efficacy of tES, or if we need to focus of spatial resolution while applying tES. This remains an empirical question. This was a motivating factor for me to

choose the large pads for the studies in this thesis over the more focal montages. I have specifically tried to investigate the mechanisms of tES, applied the way it has been most commonly used and found to be effective in the clinic and behavioral neurosciences.

This argument, however, doesn't criticize the development of customized head models for individual subjects and adjusting the placement of electrodes based on that. This will likely remove a lot of inter subject variability that is often reported in the tES literature. But as shown in chapter 3, tES effects are also dependent on the subject's internal brain state (which in our case was the inherent adaptability to a prolonged motion stimulus). Therefore equalizing the electric field distribution across subjects might not necessarily lead to similar tES effects.

6.5. Future Directions

The work presented in this thesis can be expanded on many fronts. In the subsequent sections, I will provide a gist of prospective experiments that will build upon the results presented here.

Using phosphene detection to compare different electrode montages.

In chapter 2, I provided evidence that phosphenes evoked by the application of tES over the visual cortex originate at the retina. This shows that there is a huge current spread during the application of tACS. This work has been successfully validated by a subsequent computational modelling study (Laakso and Hirata,

2013). Similar results have been observed by other groups (Schutter and Hortensius, 2010).

There has been recent attempts to improve the focality of tES by using different electrode montages (Dmochowski et al., 2011). A recent study by Kuo et al. (2013) compared the physiological effects of the conventional electrode montage (rectangular 35cm^2 pads) with the high density (HD) tDCS 4x1 ring montage (refer Figure 1.2b). They reported that HD tDCS has longer lasting effects. Future studies can be done to test the focality of tES using a high density (4x1) ring electrode configuration (Bikson et al., 2012), concentric sphere electrode montage (Datta et al., 2008) and the standard electrode montage (Utz et al., 2010). Higher current spread for any given montage should result in a lower phosphene threshold. Therefore, phosphene detection thresholds can be used as a measure of the extent of current spread, and hence serve as an index for the focality of the electrode montage.

Investigating the generalizability of the adaptation effect

Adaptation is a ubiquitous phenomenon in the mammalian cortex (Kohn, 2007). One of the major advantages of using adaptation as a tool to investigate tES mechanism is that, the anti-adaptive effect of tES should generalize across the entire cortex. Hence the same experiments can be done on areas like the primary visual cortex (area V1) with orientation adaptation or area V4 with color adaptation to check for the generalizability of the mechanism proposed in this thesis. Preliminary results from recording done with multi-electrode arrays in area V1 show that indeed tES applied at 10 Hz reduces orientation adaptation.

Concurrent tACS and fMRI

Recent studies have investigated the changes in the bold oxygenation level dependent (BOLD) signal during application of transcranial direct current stimulation (Antal et al., 2012). The method has several advantages. First, it allows researchers to look at the entire brain activity while stimulating a part of the head (Meinzer et al., 2012) and not limit the conclusion and the analysis to the area of interest. Second, it can be concurrently used with various psychophysical tasks (Huk et al., 2001). However, the method suffers from the common shortcomings of all brain imaging studies. Specifically, the ambiguous interpretation of the BOLD signal (Krekelberg et al., 2006a), the low temporal and spatial resolution of the BOLD signal and cost of performing such experiments. The work presented in this thesis can be followed up by simultaneously measuring BOLD signal while human subjects are shown visual motion adapters. A similar study has been done (Huk et al., 2001) to estimate changes in BOLD signal during motion adaptation. Future studies can use a very similar behavioral paradigm with the additional condition of applying tACS.

6.6. Final Conclusions

In this thesis, I have investigated the mechanisms of transcranial electrical stimulation. One of my primary findings is that, tES (10 Hz) applied at current densities of approximately 0.01 mA/cm^2 over the parietal cortex (area hMT+), reduces the behavioral aftereffects of visual motion adaptation. I further provide

electrophysiological evidence for this mechanism through intracortical recordings in awake, behaving macaques. Motion sensitive neurons in area MT (of the macaques) showed a similar attenuation of adaptive effects. These results bring forward a novel mechanism of tES: attenuation of adaptation. In this thesis work, I have provided sufficient electrophysiological and computational evidence supporting this speculated mechanism. A better understanding of the cellular mechanisms underlying the anti-adaptation property of tES will help optimize its use in the clinic and cognitive neuroscience.

References

Adibi M, McDonald JS, Clifford CW, Arabzadeh E (2013) Adaptation improves neural coding efficiency despite increasing correlations in variability. The Journal of neuroscience : the official journal of the Society for Neuroscience 33:2108-2120.

Akhtari M, Bryant HC, Mamelak AN, Flynn ER, Heller L, Shih JJ, Mandelkern M, Matlachov A, Ranken DM, Best ED, DiMauro MA, Lee RR, Sutherling WW (2002) Conductivities of three-layer live human skull. Brain Topography 14:151-167.

Albright TD (1984) Direction and orientation selectivity of neurons in visual area MT of the macaque. J Neurophysiol 52:1106-1130.

Ali MM, Sellers KK, Frohlich F (2013) Transcranial alternating current stimulation modulates large-scale cortical network activity by network resonance. The Journal of neuroscience. 33:11262-11275.

Antal A, Terney D, Kuhnl S, Paulus W (2010) Anodal transcranial direct current stimulation of the motor cortex ameliorates chronic pain and reduces short intracortical inhibition. Journal of pain and symptom management 39:890-903.

Antal A, Kovacs G, Chaieb L, Cziraki C, Paulus W, Greenlee MW (2012) Cathodal stimulation of human MT+ leads to elevated fMRI signal: a tDCS-fMRI study. Restorative Neurology and Neuroscience 30:255-263.

Antal A, Varga ET, Nitsche MA, Chadaide Z, Paulus W, Kovacs G, Vidnyanszky Z (2004) Direct current stimulation over MT+/V5 modulates motion aftereffect in humans. Neuroreport 15:2491-2494.

Attwell D (2003) Interaction of low frequency electric fields with the nervous system: the retina as a model system. Radiat Prot Dosimet 106:341-348.

Barlow H, Foldiak P (1989) Adaptation and decorrelation in the cortex. In: The computing neuron (Durbin R, Miall C, Mitchison G, King's College (University of Cambridge). Research Centre, eds), pp 54-72. Wokingham, England ; Reading, Mass.: Addison-Wesley Pub. Co.

Basar E, Basar-Eroglu C, Karakas S, Schurmann M (2001) Gamma, alpha, delta, and theta oscillations govern cognitive processes. International journal of psychophysiology. 39:241-248.

Baylor DA, Nunn BJ, Schnapf JL (1984) The photocurrent, noise and spectral sensitivity of rods of the monkey Macaca fascicularis. The Journal of Physiology 357:575-607.

Benardete EA, Kaplan E (1999) The dynamics of primate M retinal ganglion cells. Vis Neurosci 16:355-368.

Bikson M, Rahman A, Datta A (2012) Computational models of transcranial direct current stimulation. Clinical EEG and neuroscience. 43:176-183.

Blake R, Hiris E (1993) Another means for measuring the motion aftereffect. Vision Res 33:1589-1592.

Bolzoni F, Pettersson LG, Jankowska E (2013) Evidence for longlasting subcortical facilitation by transcranial direct current stimulation (tDCS) in the cat. The Journal of physiology. 591:3381–3399

Brindley GS (1955) The site of electrical excitation of the human eye. J Physiol 127:189-200.

Brittain JS, Probert-Smith P, Aziz TZ, Brown P (2013) Tremor suppression by rhythmic transcranial current stimulation. Current biology : CB 23:436-440.

Brunoni AR, Nitsche MA, Bolognini N, Bikson M, Wagner T, Merabet L, Edwards DJ, Valero-Cabre A, Rotenberg A, Pascual-Leone A, Ferrucci R, Priori A, Boggio PS, Fregni F (2012) Clinical research with transcranial direct current stimulation (tDCS): Challenges and future directions. Brain stimulation 5:175-195.

Buzsaki G, Anastassiou CA, Koch C (2012) The origin of extracellular fields and currents--EEG, ECoG, LFP and spikes. Nature reviews Neuroscience 13:407-420.

Carandini M, Ringach DL (1997) Predictions of a recurrent model of orientation selectivity. Vision Res 37:3061-3071.

Castet E, Keeble DR, Verstraten FA (2002) Nulling the motion aftereffect with dynamic random-dot stimuli: limitations and implications. J Vis 2:302-311.

Chaudhuri A (1990) Modulation of the motion aftereffect by selective attention. Nature 344:60-62.

Clifford CW, Webster MA, Stanley GB, Stocker AA, Kohn A, Sharpee TO, Schwartz O (2007) Visual adaptation: neural, psychological and computational aspects. Vision Res 47:3125-3131.

Cohen Kadosh R, Soskic S, Iuculano T, Kanai R, Walsh V (2010) Modulating Neuronal Activity Produces Specific and Long-Lasting Changes in Numerical Competence. Current Biology : CB 20:2016-2020.

Cronin B, Stevenson IH, Sur M, Kording KP (2010) Hierarchical Bayesian modeling and Markov chain Monte Carlo sampling for tuning-curve analysis. J Neurophysiol 103:591-602.

Datta A, Bansal V, Diaz J, Patel J, Reato D, Bikson M (2009) Gyri-precise head model of transcranial direct current stimulation: improved spatial focality using a ring electrode versus conventional rectangular pad. Brain Stimulation 2:201-207.

de Graaf TA, Gross J, Paterson G, Rusch T, Sack AT, Thut G (2013) Alpha-band rhythms in visual task performance: phase-locking by rhythmic sensory stimulation. PloS one 8:e60035.

Delbeke J, Oozeer M, Veraart C (2003) Position, size and luminosity of phosphenes generated by direct optic nerve stimulation. Vision Res 43:1091-1102.

Dmochowski JP, Datta A, Bikson M, Su Y, Parra LC (2011) Optimized multi-electrode stimulation increases focality and intensity at target. J Neural Eng 8:046011.

Duijnhouwer J, Noest AJ, Lankheet MJ, van den Berg AV, van Wezel RJ (2013) Speed and direction response profiles of neurons in macaque MT and MST show modest constraint line tuning. Frontiers in behavioral neuroscience 7:22.

Dukelow SP, DeSouza JF, Culham JC, van den Berg AV, Menon RS, Vilis T (2001) Distinguishing subregions of the human MT+ complex using visual fields and pursuit eye movements. J Neurophysiol 86:1991-2000.

Efron B, Tibshirani RJ (1994) An Introduction to the Bootstrap. Boca Raton, FL: Chapman & Hall/CRC.

Fedorov A, Chibisova Y, Szymaszek A, Alexandrov M, Gall C, Sabel BA (2010) Non-invasive alternating current stimulation induces recovery from stroke. Restorative Neurology and Neuroscience 28:825-833.

Fernandez FR, Broicher T, Truong A, White JA (2011) Membrane voltage fluctuations reduce spike frequency adaptation and preserve output gain in CA1 pyramidal neurons in a high-conductance state. The Journal of neuroscience. 31:3880-3893.

Finney DJ (1947) Probit analysis; a statistical treatment of the sigmoid response curve. Cambridge Eng.: Univ. Press.

Francis JT, Gluckman BJ, Schiff SJ (2003) Sensitivity of neurons to weak electric fields. The Journal of neuroscience. 23:7255-7261.

Fricke K, Seeber AA, Thirugnanasambandam N, Paulus W, Nitsche MA, Rothwell JC (2011) Time course of the induction of homeostatic plasticity generated by repeated transcranial direct current stimulation of the human motor cortex. J Neurophysiol 105:1141-1149.

Fritsch B, Reis J, Martinowich K, Schambra HM, Ji Y, Cohen LG, Lu B (2010) Direct current stimulation promotes BDNF-dependent synaptic plasticity: potential implications for motor learning. Neuron 66:198-204.

Furman M, Wang XJ (2008) Similarity effect and optimal control of multiple-choice decision making. Neuron 60:1153-1168.

Harris KD, Henze DA, Csicsvari J, Hirase H, Buzsaki G (2000) Accuracy of tetrode spike separation as determined by simultaneous intracellular and extracellular measurements. J Neurophysiol 84:401-414.

Hartmann TS, Bremmer F, Albright TD, Krekelberg B (2011) Receptive field positions in area MT during slow eye movements. J Neurosci 31:10437-10444.

Hecht D, Walsh V, Lavidor M (2010) Transcranial direct current stimulation facilitates decision making in a probabilistic guessing task. J Neurosci 30:4241-4245.

Helfrich RF, Schneider TR, Rach S, Trautmann-Lengsfeld SA, Engel AK, Herrmann CS (2014) Entrainment of brain oscillations by transcranial alternating current stimulation. Current Biology : CB 24:333-339.

Hermes D, Miller KJ, Wandell BA, Winawer J (2014) Stimulus Dependence of Gamma Oscillations in Human Visual Cortex. Cereb Cortex. bhu091

Herrmann CS, Rach S, Neuling T, Struber D (2013) Transcranial alternating current stimulation: a review of the underlying mechanisms and modulation of cognitive processes. Frontiers in human neuroscience 7:279.

Hiris E, Blake R (1992) Another perspective on the visual motion aftereffect. Proc Natl Acad Sci USA 89:9025-9028.

Hoffmann M, Dorn TJ, Bach M (1999) Time course of motion adaptation: motion-onset visual evoked potentials and subjective estimates. Vision Res 39:437-444.

Huk AC, Ress D, Heeger DJ (2001) Neuronal basis of the motion aftereffect reconsidered. Neuron 32:161-172.

Jefferson S, Mistry S, Singh S, Rothwell J, Hamdy S (2009) Characterizing the application of transcranial direct current stimulation in human pharyngeal motor cortex. American journal of physiology Gastrointestinal and Liver Physiology 297:G1035-1040.

Jeffreys DA, Axford JG (1972) Source locations of pattern-specific components of human visual evoked potentials. I. Component of striate cortical origin. Exp Brain Res 16:1-21.

Joundi RA, Jenkinson N, Brittain JS, Aziz TZ, Brown P (2012) Driving oscillatory activity in the human cortex enhances motor performance. Current Biology : CB 22:403-407.

Kanai R, Chaieb L, Antal A, Walsh V, Paulus W (2008) Frequency-dependent electrical stimulation of the visual cortex. Current Biology: CB 18:1839-1843.

Kar K, Krekelberg B (2012) Transcranial electrical stimulation over visual cortex evokes phosphenes with a retinal origin. J Neurophysiol 108:2173-2178.

Kar K, Wright J (2014) Probing the mechanisms underlying the mitigation of cognitive aging with anodal transcranial direct current stimulation. J Neurophysiol 111:1397-1399.

Kar K, Krekelberg B (2014) Transcranial Alternating Current Stimulation Attenuates Visual Motion Adaptation. J Neurosci 34: 7334-7340.

Kincses TZ, Antal A, Nitsche MA, Bartfai O, Paulus W (2004) Facilitation of probabilistic classification learning by transcranial direct current stimulation of the prefrontal cortex in the human. Neuropsychologia 42:113-117.

Kirov R, Weiss C, Siebner HR, Born J, Marshall L (2009) Slow oscillation electrical brain stimulation during waking promotes EEG theta activity and memory encoding. Proc Natl Acad Sci U S A 106:15460-15465.

Kohn A (2007) Visual Adaptation: Physiology, Mechanisms, and Functional Benefits. J Neurophysiol 97:3155-3164.

Kohn A, Movshon JA (2003) Neuronal Adaptation to Visual Motion in Area MT of the Macaque. Neuron 39:681-691.

Kohn A, Movshon JA (2004) Adaptation changes the direction tuning of macaque MT neurons. Nature Neurosci 7:764-772.

Kontsevich LL, Tyler CW (1999) Bayesian adaptive estimation of psychometric slope and threshold. Vision Res 39:2729-2737.

Krekelberg B (2008a) Motion Detection Mechanisms. In: The Senses: A Comprehensive Reference (Basbaum A, ed). Oxford: Elsevier Inc.

Krekelberg B (2008b) Perception of Direction is not Compensated for Neural Latency. Behavioral and Brain Science 31:208-209.

Krekelberg B, Boynton G, Vanwezel R (2006a) Adaptation: from single cells to BOLD signals. Trends Neurosci 29:250-256.

Krekelberg B, van Wezel RJ, Albright TD (2006b) Adaptation in macaque MT reduces perceived speed and improves speed discrimination. J Neurophysiol 95:255-270.

Kuo HI, Bikson M, Datta A, Minhas P, Paulus W, Kuo MF, Nitsche MA (2013) Comparing cortical plasticity induced by conventional and high-definition 4 x 1 ring tDCS: a neurophysiological study. Brain Stimulation 6:644-648.

Laakso I, Hirata A (2013) Computational analysis shows why transcranial alternating current stimulation induces retinal phosphenes. Journal of Neural Engineering 10:046009.

Laakso I, Matsumoto H, Hirata A, Terao Y, Hanajima R, Ugawa Y (2014) Multi-scale simulations predict responses to non-invasive nerve root stimulation. Journal of neural engineering 11:056013.

Liebetanz D, Nitsche MA, Tergau F, Paulus W (2002) Pharmacological approach to the mechanisms of transcranial DC-stimulation-induced after-effects of human motor cortex excitability. Brain 125:2238-2247.

Lu B (2003) BDNF and activity-dependent synaptic modulation. Learn Mem 10:86-98.

Makowiecki K, Harvey AR, Sherrard RM, Rodger J (2014) Low-intensity repetitive transcranial magnetic stimulation improves abnormal visual cortical circuit topography and upregulates BDNF in mice. The Journal of Neuroscience. 34:10780-10792.

Marshall L, Helgadottir H, Molle M, Born J (2006) Boosting slow oscillations during sleep potentiates memory. Nature 444:610-613.

Meier-Koll A (1973) [Electric stimulation of the retina in ophthalmologic differential diagnosis]. Biomedizinische Technik Biomedical engineering 18:92-97.

Meinzer M, Lindenberg R, Antonenko D, Flaisch T, Floel A (2013) Anodal transcranial direct current stimulation temporarily reverses age-associated cognitive decline and functional brain activity changes. J Neurosci 33:12470-12478.

Meinzer M, Antonenko D, Lindenberg R, Hetzer S, Ulm L, Avirame K, Flaisch T, Floel A (2012) Electrical brain stimulation improves cognitive performance by modulating functional connectivity and task-specific activation. J Neurosci 32:1859-1866.

Miranda PC, Lomarev M, Hallett M (2006) Modeling the current distribution during transcranial direct current stimulation. Clinical Neurophysiology 117:1623-1629.

Newsome WT, Pare EB (1988) A selective impairment of motion perception following lesions of the middle temporal visual area (MT). J Neurosci 8:2201-2211.

Nishida S (2011) Advancement of motion psychophysics: review 2001-2010. J Vis 11:11.

Nitsche MA, Paulus W (2000) Excitability changes induced in the human motor cortex by weak transcranial direct current stimulation. Journal of Physiology 527:633-639.

Nitsche MA, Paulus W (2001) Sustained excitability elevations induced by transcranial DC motor cortex stimulation in humans. Neurology 57:1899-1901.

Nitsche MA, Liebetanz D, Tergau F, Paulus W (2002) [Modulation of cortical excitability by transcranial direct current stimulation]. Nervenarzt 73:332-335.

Nitsche MA, Fricke K, Henschke U, Schlitterlau A, Liebetanz D, Lang N, Henning S, Tergau F, Paulus W (2003) Pharmacological modulation of cortical excitability shifts induced by transcranial direct current stimulation in humans. Journal of Physiology 553:293-301.

Nitsche MA, Cohen LG, Wassermann EM, Priori A, Lang N, Antal A, Paulus W, Hummel F, Boggio PS, Fregni F, Pascual-Leone A (2008) Transcranial

direct current stimulation: State of the art 2008. Brain Stimulation 1:206-223.

Nitsche MA, Seeber A, Frommann K, Klein CC, Rochford C, Nitsche MS, Fricke K, Liebetanz D, Lang N, Antal A, Paulus W, Tergau F (2005) Modulating parameters of excitability during and after transcranial direct current stimulation of the human motor cortex. Journal of Physiology 568:291-303.

Orban GA, Fize D, Peuskens H, Denys K, Nelissen K, Sunaert S, Todd J, Vanduffel W (2003) Similarities and differences in motion processing between the human and macaque brain: evidence from fMRI. Neuropsychologia 41:1757-1768.

Ozen S, Sirota A, Belluscio MA, Anastassiou CA, Stark E, Koch C, Buzsaki G (2010) Transcranial electric stimulation entrains cortical neuronal populations in rats. J Neurosci 30:11476-11485.

Palm U, Keeser D, Schiller C, Fintescu Z, Reisinger E, Baghai TC, Mulert C, Padberg F (2009) Transcranial direct current stimulation in a patient with therapy-resistant major depression. World J Biol Psychiatry 10:632-635.

Parker AJ, Newsome WT (1998) Sense and the Single Neuron: Probing the Physiology of Perception. Annu Rev Neurosci 21:227-277.

Patterson CA, Wissig SC, Kohn A (2013) Distinct effects of brief and prolonged adaptation on orientation tuning in primary visual cortex. J Neurosci 33:532-543.

Patterson CA, Duijnhouwer J, Wissig SC, Krekelberg B, Kohn A (2014) Similar adaptation effects in primary visual cortex and area MT of the macaque monkey under matched stimulus conditions. J Neurophysiol 111:1203-1213.

Paulus W (2010) On the difficulties of separating retinal from cortical origins of phosphenes when using transcranial alternating current stimulation (tACS). Clin Neurophysiol 121:987-991.

Pfurtscheller G, Stancak A, Jr., Neuper C (1996) Event-related synchronization (ERS) in the alpha band--an electrophysiological correlate of cortical idling: a review. International journal of psychophysiology : official journal of the International Organization of Psychophysiology 24:39-46.

Piantoni G, Kline KA, Eagleman DM (2010) Beta oscillations correlate with the probability of perceiving rivalrous visual stimuli. J Vis 10:18.

Polania R, Nitsche MA, Korman C, Batsikadze G, Paulus W (2012) The Importance of Timing in Segregated Theta Phase-Coupling for Cognitive Performance. Current biology : CB.

Priori A, Berardelli A, Rona S, Accornero N, Manfredi M (1998) Polarization of the human motor cortex through the scalp. Neuroreport 9:2257-2260.

Purpura K, Tranchina D, Kaplan E, Shapley RM (1990) Light adaptation in the primate retina: analysis of changes in gain and dynamics of monkey retinal ganglion cells. Vis Neurosci 4:75-93.

Radman T, Ramos RL, Brumberg JC, Bikson M (2009) Role of cortical cell type and morphology in subthreshold and suprathreshold uniform electric field stimulation in vitro. Brain Stimulation 2:215-228.

Reato D, Rahman A, Bikson M, Parra LC (2010) Low-intensity electrical stimulation affects network dynamics by modulating population rate and spike timing. J Neurosci 30:15067-15079.

Reato D, Rahman A, Bikson M, Parra LC (2013) Effects of weak transcranial alternating current stimulation on brain activity-a review of known mechanisms from animal studies. Frontiers in human neuroscience 7:687.

Reppas JB, Newsome WT (2007) Brain stimulation: feeling the buzz. Curr Biol 17:R358-360.

Rezec A, Krekelberg B, Dobkins KR (2004) Attention enhances adaptability: evidence from motion adaptation experiments. Vision Res 44:3035-3044.

Richert M, Albright TD, Krekelberg B (2013) The complex structure of receptive fields in the middle temporal area. Front Syst Neurosci 7:2.

Rohracher H (1935) Uber subjektive Lichterscheinungen bei Reizung mit Wechselstromen Zeitschrift für Sinnesphysiologie 66:164-181.

Rosenkranz K, Nitsche MA, Tergau F, Paulus W (2000) Diminution of training-induced transient motor cortex plasticity by weak transcranial direct current stimulation in the human. Neurosci Lett 296:61-63.

Sanchez-Vives MV, Nowak LG, McCormick DA (2000a) Cellular mechanisms of long-lasting adaptation in visual cortical neurons in vitro. The Journal of Neuroscience : the official journal of the Society for Neuroscience 20:4286-4299.

Sanchez-Vives MV, Nowak LG, McCormick DA (2000b) Membrane mechanisms underlying contrast adaptation in cat area 17 in vivo. J Neurosci 20:4267-4285.

Scase MO, Braddick OJ, Raymond JE (1996) What is noise for the motion system? Vision Res 36:2579-2586.

Schlaug G, Renga V, Nair D (2008) Transcranial direct current stimulation in stroke recovery. Arch Neurol 65:1571-1576.

Schneeweis DM, Schnapf JL (1999) The photovoltage of macaque cone photoreceptors: adaptation, noise, and kinetics. The Journal of neuroscience : the official journal of the Society for Neuroscience 19:1203-1216.

Schoppmann A, Hoffmann KP (1976) Continuous mapping of direction selectivity in the cat's visual cortex. Neurosci Lett 2:177-181.

Schutter DJ, Hortensius R (2010) Retinal origin of phosphenes to transcranial alternating current stimulation. Clin Neurophysiol 121:1080-1084.

Schwiedrzik CM (2009) Retina or visual cortex? The site of phosphene induction by transcranial alternating current stimulation. Front Integr Neurosci 3:6.

Sela T, Kilim A, Lavidor M (2012) Transcranial alternating current stimulation increases risk-taking behavior in the balloon analog risk task. Front Neurosci 6:22.

Spigel IM (1964) The Use of Decay Inhibition in an Examination of Central Mediation in Movement Aftereffects. J Gen Psychol 70:241-247.

Stecker MM (2005) Transcranial electric stimulation of motor pathways: a theoretical analysis. Comput Biol Med 35:133-155.

Stroud AC, Ledue EE, Crowder NA (2012) Orientation specificity of contrast adaptation in mouse primary visual cortex. J Neurophysiol 108:1381-1391.

Struber D, Rach S, Trautmann-Lengsfeld SA, Engel AK, Herrmann CS (2014) Antiphasic 40 Hz oscillatory current stimulation affects bistable motion perception. Brain Topography 27:158-171.

Sunaert S, Van Hecke P, Marchal G, Orban GA (1999) Motion-responsive regions of the human brain. Experimental brain research Experimentelle Hirnforschung Experimentation cerebrale 127:355-370.

Terney D, Chaieb L, Moliadze V, Antal A, Paulus W (2008) Increasing human brain excitability by transcranial high-frequency random noise stimulation. The Journal of neuroscience : the official journal of the Society for Neuroscience 28:14147-14155.

Turi Z, Ambrus GG, Janacsek K, Emmert K, Hahn L, Paulus W, Antal A (2013) Both the cutaneous sensation and phosphene perception are modulated in a frequency-specific manner during transcranial alternating current stimulation. Restorative neurology and neuroscience 31:275-285.

Utz KS, Dimova V, Oppenlander K, Kerkhoff G (2010) Electrified minds: transcranial direct current stimulation (tDCS) and galvanic vestibular stimulation (GVS) as methods of non-invasive brain stimulation in neuropsychology--a review of current data and future implications. Neuropsychologia 48:2789-2810.

Van Wezel RJ, Britten KH (2002) Motion adaptation in area MT. J Neurophysiol 88:3469-3476.

Victor JD (1987) The dynamics of the cat retinal X cell centre. J Physiol 386:219-246.

Voss U, Holzmann R, Hobson A, Paulus W, Koppehele-Gossel J, Klimke A, Nitsche MA (2014) Induction of self awareness in dreams through frontal low current stimulation of gamma activity. Nature Neurosci 17:810-812.

Vul E, Krizay E, MacLeod DI (2008) The McCollough effect reflects permanent and transient adaptation in early visual cortex. J Vis 8:4 1-12.

Wang XJ, Liu Y, Sanchez-Vives MV, McCormick DA (2003) Adaptation and temporal decorrelation by single neurons in the primary visual cortex. J Neurophysiol 89:3279-3293.

Wissig SC, Kohn A (2012) The influence of surround suppression on adaptation effects in primary visual cortex. J Neurophysiol 107:3370-3384.

Yamamoto Y, Struzik ZR, Soma R, Ohashi K, Kwak S (2005) Noisy vestibular stimulation improves autonomic and motor responsiveness in central neurodegenerative disorders. Ann Neurol 58:175-181.

Zaghi S, Acar M, Hultgren B, Boggio PS, Fregni F (2010) Noninvasive brain stimulation with low-intensity electrical currents: putative mechanisms of action for direct and alternating current stimulation. Neuroscientist 16:285-307.

Vita

1985 Born September 16 in Kolkata, India

2004 Graduated from W.W.A Cossipore English School (High School), Kolkata, India

2008 Bachelor of Technology in Electronics and Instrumentation Engineering , West Bengal University of Technology (Heritage Institute of Technology), Kolkata, India

2010 MS in Biomedical Engineering, New Jersey Institute of Technology, New Jersey, USA

2010 **Kar, K.**, Moustafa A, Myers C, Gluck M: Using an animal learning model of the hippocampus to simulate human fMRI data. Bioengineering Conference, *Proceedings of the 2010 IEEE 36th Annual Northeast ,* vol., no., pp.1-2, 26-28

2011 **Kar, K.**, Krekelberg B: Retinal and cortical effects of transcranial electric stimulation. *Journal of Vision 2011*, VSS Abstracts.

2012 **Kar, K.**, Krekelberg B: Effects of transcranial electrical stimulation on human motion detection. *Journal of Vision* 2012, VSS Abstracts.

2012 **Kar, K.**, Krekelberg, B: "Transcranial electrical stimulation over visual cortex evokes phosphenes with a retinal origin." *Journal of Neurophysiology* (2012).

2013 **Kar, K.,** Duijnhouwer, J. and Krekelberg, B: Transcranial electrical stimulation affects adaptation of MT/V5 neurons in awake behaving macaques. *Journal of Vision* 2013, VSS abstracts

2013 **Kar, K.,** Duijnhouwer, J. and Krekelberg, B: Transcranial alternating current stimulation affects motion adaptation in V1 and MT neurons in awake, behaving macaques. *Rhythmic Dynamics and Cognition Conference, 2013*

2013 **Kar, K.**, Duijnhouwer, J, Krekelberg, B: Transcranial electrical stimulation mitigates motion adaptation in V1, MT, and MST neurons of awake, behaving macaques. *Neuroscience 2013* Abstracts. San Diego, CA: Society for Neuroscience, 2013

2014 **Kar, K**., and Wright, J: "Probing the mechanisms underlying the mitigation of cognitive aging with anodal transcranial direct current stimulation." *Journal of Neurophysiology* (2014).

2014 **Kar, K.**, Duijnhouwer, J, and Krekelberg, B: "tACS-What goes on inside? The neural consequences of transcranial alternating current stimulation." *Brain Stimulation* 7.2 (2014): e12.

2014 **Kar, K.** and Krekelberg B: "Transcranial alternating current stimulation attenuates visual motion adaptation." *Journal of Neuroscience* (2014).

2014 Sip, K.E, Smith, D.V, Porcelli, A.J., **Kar**, **K.**, Delgado, M.R: "Social closeness and feedback modulate susceptibility to the framing effect." *Social Neuroscience* (2014)

2015 PhD in Neuroscience